Constraints on anomalous *HVV* couplings from the production of Higgs bosons decaying to τ lepton pairs

A. M. Sirunyan *et al.*[*]

(CMS Collaboration)

A study is presented of anomalous *HVV* interactions of the Higgs boson, including its *CP* properties. The study uses Higgs boson candidates produced mainly in vector boson fusion and gluon fusion that subsequently decay to a pair of τ leptons. The data were recorded by the CMS experiment at the LHC in 2016 at a center-of-mass energy of 13 TeV and correspond to an integrated luminosity of 35.9 fb^{-1}. A matrix element technique is employed for the analysis of anomalous interactions. The results are combined with those from the $H \to 4\ell$ decay channel presented earlier, yielding the most stringent constraints on anomalous Higgs boson couplings to electroweak vector bosons expressed as effective cross section fractions and phases: the *CP*-violating parameter $f_{a3}\cos(\phi_{a3}) = (0.00 \pm 0.27) \times 10^{-3}$ and the *CP*-conserving parameters $f_{a2}\cos(\phi_{a2}) = (0.08^{+1.04}_{-0.21}) \times 10^{-3}$, $f_{\Lambda1}\cos(\phi_{\Lambda1}) = (0.00^{+0.53}_{-0.09}) \times 10^{-3}$, and $f^{Z\gamma}_{\Lambda1}\cos(\phi^{Z\gamma}_{\Lambda1}) = (0.0^{+1.1}_{-1.3}) \times 10^{-3}$. The current dataset does not allow for precise constraints on *CP* properties in the gluon fusion process. The results are consistent with standard model expectations.

I. INTRODUCTION

The Higgs boson (*H*) discovered in 2012 at the CERN LHC [1–3] has thus far been found to have properties consistent with expectations from the standard model (SM) [4–10]. In particular, its spin-parity quantum numbers are consistent with $J^{PC} = 0^{++}$ according to measurements performed by the CMS [11–17] and ATLAS [18–23] experiments. It is still to be determined whether small anomalous couplings contribute to the *HVV* or *Hff* interactions, where *V* stands for vector bosons and f stands for fermions. Because nonzero spin assignments of the *H* boson have been excluded [13,19], we focus on the analysis of couplings of a spin-0 *H* boson. Previous studies of anomalous *HVV* couplings were performed by both the CMS and ATLAS experiments using either decay-only information [11–13,18,19,21], including associated production information [15–17,20,22,23], or including off-shell *H* boson production [14,17]. In this paper, we report a study of *HVV* couplings using information from production of the *H* boson decaying to τ leptons. These results are combined with the previous CMS measurements using both associated production and decay information in the $H \to 4\ell$ channel [17],

resulting in stringent constraints on anomalous *H* boson couplings. Here and in the following, ℓ denotes an electron or muon.

The $H \to \tau\tau$ decay has been observed by the CMS experiment, with over five standard deviation significance [24]. The $H \to \tau\tau$ sample can be used to study the quantum numbers of the *H* boson and its anomalous couplings to SM particles, including its *CP* properties. The dominant production mechanisms of the *H* boson considered in this paper are shown at leading order in QCD in Fig. 1. Anomalous *HWW*, *HZZ*, *HZγ*, *Hγγ*, and *Hgg* couplings affect the correlations between the *H* boson, the beam line direction, and the two jets in vector boson fusion (VBF), in associated production with a vector boson decaying hadronically (*VH*, where $V = W$; *Z*), or gluon fusion production with an additional two jets. The gluon fusion production with two additional jets appears at higher order in QCD with an example of gluons appearing in place of the vector bosons shown in the VBF diagram in the middle of Fig. 1. A study of anomalous $Ht\bar{t}$ couplings in associated production with top quarks, $t\bar{t}H$ or tqH, and anomalous $H\tau\tau$ couplings in the decay of the *H* boson are also possible using $\tau\tau$ events [25]. However, more data are needed to reach sensitivity to such anomalous effects, and it has been confirmed that these anomalous couplings would not affect the measurements presented in this paper.

To increase the sensitivity to anomalous couplings in the *H* boson production, the matrix element likelihood approach (MELA) [2,26–29] is utilized to form optimal observables. The analysis is optimized for VBF production

---

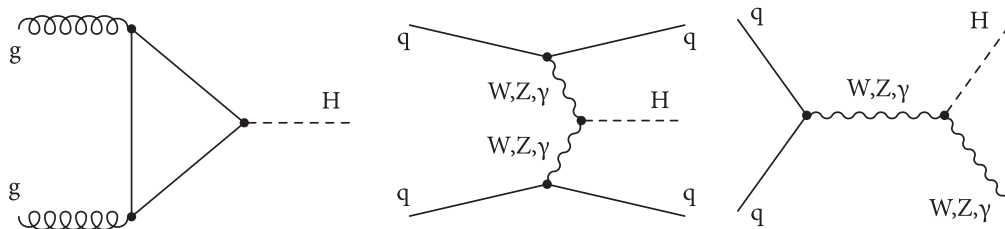[*]Full author list given at the end of the article.

FIG. 1. Examples of leading-order Feynman diagrams for H boson production via the gluon fusion (left), vector boson fusion (middle), and associated production with a vector boson (right). The HWW and HZZ couplings may appear at tree level, as the SM predicts. Additionally, HWW, HZZ, $HZ\gamma$, $H\gamma\gamma$, and Hgg couplings may be generated by loops of SM or unknown particles, as indicated in the left diagram but not shown explicitly in the middle and right diagrams.

and is not additionally optimized for VH or gluon fusion production. However, all three production mechanisms are included in the analysis, using a general anomalous coupling parametrization. The $H \to \tau\tau$ channel has advantages over other H boson decay channels because of the relatively high significance of the signal events in the VBF channel [24]. Three mutually exclusive categories of events are reconstructed in the analysis: the VBF category targets events with two associated jets in the VBF event topology, the boosted category contains events with one jet or more jets if the event is not in the VBF category, and the 0-jet category targets H boson events produced via gluon fusion without associated jets. The simultaneous analysis of all three categories of events is necessary to boost the sensitivity to anomalous HVV couplings from events with partial kinematic information reconstructed in the non-VBF categories and to normalize the relative contribution of different production mechanisms.

The analysis utilizes the same data, event selection, and categorization as Ref. [24] and is described in Sec. III. The phenomenological model and Monte Carlo (MC) simulation are described in Sec. IV. The matrix element techniques used to extract the kinematic information are discussed in Sec. V. The implementation of the likelihood fit using kinematic information in the events is presented in Sec. VI. The results are presented and discussed in Secs. VII and VIII, before conclusions are drawn in Sec. IX.

II. CMS DETECTOR

The central feature of the CMS apparatus is a superconducting solenoid of 6 m internal diameter, providing a magnetic field of 3.8 T. Within the solenoid volume, there are a silicon pixel and strip tracker, a lead tungstate crystal electromagnetic calorimeter (ECAL), and a brass and scintillator hadron calorimeter, each composed of a barrel and two end cap sections. Forward calorimeters extend the pseudorapidity, η, coverage provided by the barrel and end cap detectors. Muons are detected in gas-ionization chambers embedded in the steel flux-return yoke outside the solenoid.

Events of interest are selected using a two-tiered trigger system [30]. The first level (L1), composed of custom hardware processors, uses information from the calorimeters and muon detectors to select events at a rate of around 100 kHz within a time interval of less than 4 μs. The second level, known as the high-level trigger, consists of a farm of processors running a version of the full event reconstruction software optimized for fast processing and reduces the event rate to about 1 kHz before data storage.

A more detailed description of the CMS detector, together with a definition of the coordinate system used and the relevant kinematic variables, can be found in Ref. [31].

The data samples used in this analysis correspond to an integrated luminosity of 35.9 fb^{-1} collected in Run 2 of the LHC during 2016 at a center-of-mass energy of 13 TeV.

III. EVENT RECONSTRUCTION AND SELECTION

The analysis uses the same dataset, event reconstruction, and selection criteria as those used in the analysis leading to the observation of the H boson decay to a pair of τ leptons [24].

A. Event reconstruction

The reconstruction of observed and simulated events relies on the particle-flow (PF) algorithm [32], which combines the information from the CMS subdetectors to identify and reconstruct particles emerging from pp collisions. Combinations of these PF candidates are used to reconstruct higher-level objects such as jets, τ candidates, or missing transverse momentum, $\vec{p}_{\mathrm{T}}^{\mathrm{miss}}$. The reconstructed vertex with the largest value of summed physics object p_{t}^2 is taken to be the primary pp interaction vertex, where p_{T} is the transverse momentum. The physics objects are the objects constructed by a jet finding algorithm [33,34] applied to all charged tracks associated with the vertex and the corresponding associated missing transverse momentum.

Electrons are identified with a multivariate discriminant combining several quantities describing the track quality, the shape of the energy deposits in the ECAL, and the

compatibility of the measurements from the tracker and the ECAL [35]. Muons are identified with requirements on the quality of the track reconstruction and on the number of measurements in the tracker and the muon systems [36]. To reject nonprompt or misidentified leptons, an isolation requirement I^{ℓ} is applied according to the criteria described in Ref. [24].

Jets are reconstructed with an anti-k_T clustering algorithm [37], as implemented in the FASTJET package [34]. It is based on the clustering of neutral and charged PF candidates within a distance parameter of 0.4. Charged PF candidates not associated with the primary vertex of the interaction are not considered when building jets. An offset correction is applied to jet energies to take into account the contribution from additional pp interactions within the same or nearby bunch crossings. In this analysis, jets are required to have $p_T > 30$ GeV and absolute pseudorapidity $|\eta| < 4.7$ and to be separated from the selected leptons by a distance parameter $\Delta R = \sqrt{(\Delta\eta)^2 + (\Delta\phi)^2}$ of at least 0.5, where ϕ is the azimuthal angle in radians. The combined secondary vertex algorithm is used to identify jets that are likely to originate from a bottom quark ("b jets"). The algorithm exploits track-based lifetime information along with the secondary vertex of the jet to provide a likelihood ratio discriminator for b jet identification.

Hadronically decaying τ leptons, denoted as τ_h, are reconstructed with the hadron-plus-strips algorithm [38,39], which is seeded with anti-k_T jets. This algorithm reconstructs τ_h candidates based on the number of tracks and the number of ECAL strips with energy deposits within the associated η-ϕ plane and reconstructs one-prong, one-prong $+ \pi^0$ (s), and three-prong decay modes, identified as $M = 1, 2,$ and 3, respectively. A multivariate discriminator, including isolation and lifetime information, is used to reduce the rate for quark- and gluon-initiated jets to be identified as τ_h candidates. The working point used in this analysis has an efficiency of about 60% for genuine τ_h, with about 1% misidentification rate for quark- and gluon-initiated jets, for a p_T range typical of τ_h originating from a Z boson. Electrons and muons misidentified as τ_h candidates are suppressed using dedicated criteria based on the consistency between the measurements in the tracker, the calorimeters, and the muon detectors [38,39]. The τ_h energy scale as well as the rate and the energy scale of electrons and muons misidentified as τ_h candidates are corrected in simulation to match those measured in data [24].

The missing transverse momentum is defined as the negative vector sum of the transverse momenta of all PF candidates [40]. The details of the corrections to $\vec{p}_T^{\text{miss}}$ for the mismodeling in the simulation of $Z +$ jets, $W +$ jets, and H boson processes are described in Ref. [24].

Both the visible mass of the $\tau\tau$ system m_{vis} and the invariant mass of the $\tau\tau$ system $m_{\tau\tau}$ are used in the analysis. The visible mass is defined as the invariant mass of the

visible decay products of the τ leptons. The observable $m_{\tau\tau}$ is reconstructed using the SVFIT [41] algorithm, which combines the $\vec{p}_T^{\text{miss}}$ and its uncertainty with the 4-vectors of both τ candidates to calculate a more accurate estimate of the mass of the parent boson. The estimate of the 4-momentum of the H boson provided by SVFIT is used to calculate the kinematic observables discussed in Sec. V.

B. Event selection and categorization

Selected events are classified according to four decay channels, $e\mu$, $e\tau_h$, $\mu\tau_h$, and $\tau_h\tau_h$. The resulting event samples are made mutually exclusive by discarding events that have additional loosely identified and isolated electrons or muons.

The largest irreducible source of background is Drell-Yan production of $Z \to \tau\tau$, while the dominant background sources with jets misidentified as leptons are QCD multijet and $W +$ jets. Other contributing background sources are $t\bar{t}$, single top, $Z \to \ell\ell$, and diboson production.

The two leptons assigned to the H boson decay are required to have opposite charges. The trigger requirements, geometrical acceptances, and transverse momentum criteria are summarized in Table I. The p_T thresholds in the lepton selections are optimized to increase the sensitivity to the $H \to \tau\tau$ signal, while also satisfying the trigger requirements. The pseudorapidity requirements are driven by reconstruction and trigger requirements.

In the $\ell\tau_h$ channels, the large $W +$ jets background is reduced by requiring the transverse mass, m_T, to be less than 50 GeV. The transverse mass is defined as follows,

TABLE I. Kinematic selection criteria for the four decay channels. For the trigger threshold requirements, the numbers indicate the trigger thresholds in GeV. The lepton selection criteria include the transverse momentum threshold, pseudorapidity range, as well as isolation criteria.

	Trigger requirement	Lepton selection	
Channel	p_T (GeV)	p_T (GeV)	η
$e\mu$	$p_T^e > 12$ & $p_T^{\mu} > 23$	$p_T^e > 13$	$|\eta^e| < 2.5$
		$p_T^{\mu} > 24$	$|\eta^{\mu}| < 2.4$
	$p_T^e > 23$ & $p_T^{\mu} > 8$	$p_T^e > 24$	$|\eta^e| < 2.5$
		$p_T^{\mu} > 15$	$|\eta^{\mu}| < 2.4$
$e\tau_h$	$p_T^e > 25$	$p_T^e > 26$	$|\eta^e| < 2.1$
		$p_T^{\tau_h} > 30$	$|\eta^{\tau_h}| < 2.3$
$\mu\tau_h$	$p_T^{\mu} > 22$	$p_T^{\mu} > 23$	$|\eta^{\mu}| < 2.1$
		$p_T^{\tau_h} > 30$	$|\eta^{\tau_h}| < 2.3$
	$p_T^{\mu} > 19$ & $p_T^{\tau_h} > 21$	$20 < p_T^{\mu} < 23$	$|\eta^{\mu}| < 2.1$
		$p_T^{\tau_h} > 30$	$|\eta^{\tau_h}| < 2.3$
$\tau_h\tau_h$	$p_T^{\tau_h} > 35$ & 35	$p_T^{\tau_h} > 50$ & 40	$|\eta^{\tau_h}| < 2.1$

$$m_T \equiv \sqrt{2p_T^\ell p_T^{\text{miss}}[1 - \cos(\Delta\phi)]}, \qquad (1)$$

where p_T^ℓ is the transverse momentum of the electron or muon and $\Delta\phi$ is the azimuthal angle between the lepton direction and the $\vec{p}_T^{\text{miss}}$ direction.

In the $e\mu$ channel, the $t\bar{t}$ background is reduced by requiring $p_\zeta - 0.85p_\zeta^{\text{vis}} > -35$ GeV or -10 GeV depending on the category, where p_ζ is the component of $\vec{p}_T^{\text{miss}}$ along the bisector of the transverse momenta of the two leptons and p_ζ^{vis} is the sum of the components of the lepton transverse momenta along the same direction [42]. In addition, events with a b-tagged jet are discarded to further suppress the $t\bar{t}$ background in this channel.

In the same way as in Ref. [24], the event samples are split into three mutually exclusive production categories:

(i) 0-jet category: This category targets H boson events produced via gluon fusion. Events containing no jets with $p_T > 30$ GeV are selected. Simulations indicate that about 98% of signal events in the 0-jet category arise from the gluon fusion production mechanism.

(ii) VBF category: This category targets H boson events produced via the VBF process. Events are selected with exactly (at least) two jets with $p_T > 30$ GeV in the $e\mu$ ($e\tau_h$, $\mu\tau_h$, and $\tau_h\tau_h$) channels. In the $\mu\tau_h$, $e\tau_h$, and $e\mu$ channels, the two leading jets are required to have an invariant mass, m_{JJ}, larger than 300 GeV. The vector sum of the $\vec{p}_T^{\text{miss}}$ and the $\vec{p}_T$ of the visible decay products of the tau leptons, defined as $\vec{p}_T^{\tau\tau}$, is required to have a magnitude greater than 50 (100) GeV in the $\ell\tau_h$ ($\tau_h\tau_h$) channels. In addition, the p_T threshold on the τ_h candidate is raised to 40 GeV in the $\mu\tau_h$ channel, and the two leading jets in the $\tau_h\tau_h$ channel must be separated in pseudorapidity by $|\Delta\eta| > 2.5$. Depending on the decay channel, up to 57% of the signal events in the VBF category is produced via VBF. This fraction increases with m_{JJ}. Gluon fusion production makes 40%–50% of the total signal, while the VH contribution is less than 3%.

(iii) Boosted category: This category contains all the events that do not enter one of the previous categories, namely events with one jet and events with several jets that fail the requirements of the VBF category. It targets events with a H boson produced in gluon fusion and recoiling against an initial state radiation jet. It contains gluon fusion events produced in association with one or more jets (78%–80% of the signal events), VBF events in which one of the jets has escaped detection or events with low m_{JJ} (11%–13%), as well as H boson events produced in association with a W or a Z boson decaying hadronically (4%–8%).

In addition to these three signal regions for each channel, a series of control regions targeting different background processes are included in the maximum likelihood fit used to extract the results of the analysis. The normalization of the W + jets background in the $e\tau_h$ and $\mu\tau_h$ channels is estimated from simulations and adjusted to data using control regions obtained by applying all selection criteria, with the exception that m_T is required to be greater than 80 GeV instead of less than 50 GeV. An uncertainty on the extrapolation from the control region to the signal region is determined in the same way as described in Ref. [24]. The normalization of the QCD multijet background in the $e\tau_h$ and $\mu\tau_h$ channels is estimated from events where the electron or the muon has the same charge as the τ_h candidate. The contributions from Drell–Yan, $t\bar{t}$, diboson, and W + jets processes are subtracted. The factor to extrapolate from the same-sign to the opposite-sign region is determined by comparing the yield of the QCD multijet background for events with ℓ candidates passing inverted isolation criteria, in the same-sign and opposite-sign regions. It is constrained by adding the opposite-sign region, where the ℓ candidates pass inverted isolation criteria, to the global fit.

In the $\tau_h\tau_h$ channel, the QCD multijet background is estimated from events where the τ_h candidates pass relaxed isolation conditions, and the extrapolation factor is derived from events where the τ_h candidates have charges of the same sign. The events selected with opposite-sign τ_h candidates passing relaxed isolation requirements form a control region included in the global fit. Finally, the normalization of the $t\bar{t}$ background is adjusted using a control region defined similarly to the $e\mu$ signal region, except that the p_ζ requirement is inverted and the events are required to contain at least one jet.

IV. PHENOMENOLOGY OF ANOMALOUS COUPLINGS AND SIMULATION

We follow the formalism used in the study of anomalous couplings in earlier analyses by CMS [11–17]. The theoretical approach is described in Refs. [26–29,43–51]. Anomalous interactions of a spin-0 H boson with two spin-1 gauge bosons VV, such as WW, ZZ, $Z\gamma$, $\gamma\gamma$, and gg, are parametrized by a scattering amplitude that includes three tensor structures with expansion of coefficients up to (q^2/Λ^2)

$$A(HVV) \sim \left[a_1^{VV} + \frac{\kappa_1^{VV}q_1^2 + \kappa_2^{VV}q_2^2}{(\Lambda_1^{VV})^2}\right]m_{V1}^2\epsilon_{V1}^*\epsilon_{V2}^* + a_2^{VV}f_{\mu\nu}^{*(1)}f^{*(2)\mu\nu} + a_3^{VV}f_{\mu\nu}^{*(1)}\tilde{f}^{*(2)\mu\nu}, \qquad (2)$$

where q_i, ϵ_{Vi}, and m_{V1} are the 4-momentum, polarization vector, and pole mass of the gauge boson, indexed by $i = 1$, 2. The gauge boson's field strength tensor and dual field strength tensor are $f^{(i)\mu\nu} = \epsilon_{Vi}^\mu q_i^\nu - \epsilon_{Vi}^\nu q_i^\mu$ and $\tilde{f}_{\mu\nu}^{(i)} = \frac{1}{2}\epsilon_{\mu\nu\rho\sigma}f^{(i)\rho\sigma}$. The coupling coefficients a_i^{VV}, which

multiply the three tensor structures, and $\kappa_i^{VV}/(\Lambda_1^{VV})^2$, which multiply the next term in the q^2 expansion for the first tensor structure, are to be determined from data, where Λ_1 is the scale of beyond the SM (BSM) physics.

In Eq. (2), the only nonzero SM contributions at tree level are a_1^{WW} and a_1^{ZZ}, which are assumed to be equal under custodial symmetry. All other ZZ and WW couplings are considered anomalous contributions, which are either due to BSM physics or small contributions arising in the SM due to loop effects and are not accessible with the current precision. As the event kinematics of the H boson production in WW fusion and in ZZ fusion are very similar, they are analyzed together assuming $a_i^{WW} = a_i^{ZZ}$ and $\kappa_i^{ZZ}/(\Lambda_1^{ZZ})^2 = \kappa_i^{WW}/(\Lambda_1^{WW})^2$. The results can be reinterpreted for any other relationship between the a_i^{WW} and a_i^{ZZ} couplings [17]. For convenience, we refer to these parameters as a_i, κ_i, and Λ_1, without the superscripts. Among the anomalous contributions, considerations of symmetry and gauge invariance require $\kappa_1^{ZZ} = \kappa_2^{ZZ} = -\exp(i\phi_{\Lambda1}^{ZZ})$, $\kappa_1^{\gamma\gamma} = \kappa_2^{\gamma\gamma} = 0$, $\kappa_1^{gg} = \kappa_2^{gg} = 0$, $\kappa_1^{Z\gamma} = 0$, and $\kappa_2^{Z\gamma} = -\exp(i\phi_{\Lambda1}^{Z\gamma})$, where $\phi_{\Lambda1}^{VV}$ is the phase of the corresponding coupling. In the case of the $\gamma\gamma$ and gg couplings,

the only contributing terms are $a_2^{\gamma\gamma,gg}$ and $a_3^{\gamma\gamma,gg}$. Our earlier measurements in Ref. [13] indicated substantially tighter limits on $a_2^{\gamma\gamma,Z\gamma}$ and $a_3^{\gamma\gamma,Z\gamma}$ couplings from $H \to Z\gamma$ and $H \to \gamma\gamma$ decays with on-shell photons than from measurements with virtual photons, so we do not pursue measurements of these parameters in this paper. The coupling a_2^{gg} refers to a SM-like contribution in the gluon fusion process, and a_3^{gg} corresponds to a CP-odd anomalous contribution. There are four other anomalous couplings targeted in this analysis: two from the first term of Eq. (2), $\Lambda_1^{ZZ} = \Lambda_1^{WW} = \Lambda_1$ and $\Lambda_1^{Z\gamma}$; one coming from the second term, $a_2^{ZZ} = a_2^{WW} = a_2$; and one coming from the third term, $a_3^{ZZ} = a_3^{WW} = a_3$. The a_3 coupling corresponds to the CP-odd amplitude, and its interference with a CP-even amplitude would result in CP violation.

It is convenient to measure the effective cross section ratios f_{ai} rather than the anomalous couplings a_i themselves, as most uncertainties cancel in the ratio. Moreover, the effective fractions are conveniently bounded between 0 and 1, independent of the coupling convention. The effective fractional cross sections f_{ai} and phases ϕ_{ai} are defined as follows,

$$f_{a3} = \frac{|a_3|^2\sigma_3}{|a_1|^2\sigma_1 + |a_2|^2\sigma_2 + |a_3|^2\sigma_3 + \tilde{\sigma}_{\Lambda1}/(\Lambda_1)^4 + \cdots}, \qquad \phi_{a3} = \arg\left(\frac{a_3}{a_1}\right),$$

$$f_{a2} = \frac{|a_2|^2\sigma_2}{|a_1|^2\sigma_1 + |a_2|^2\sigma_2 + |a_3|^2\sigma_3 + \tilde{\sigma}_{\Lambda1}/(\Lambda_1)^4 + \cdots}, \qquad \phi_{a2} = \arg\left(\frac{a_2}{a_1}\right),$$

$$f_{\Lambda1} = \frac{\tilde{\sigma}_{\Lambda1}/(\Lambda_1)^4}{|a_1|^2\sigma_1 + |a_2|^2\sigma_2 + |a_3|^2\sigma_3 + \tilde{\sigma}_{\Lambda1}/(\Lambda_1)^4 + \cdots}, \qquad \phi_{\Lambda1},$$

$$f_{\Lambda1}^{Z\gamma} = \frac{\tilde{\sigma}_{\Lambda1}^{Z\gamma}/(\Lambda_1^{Z\gamma})^4}{|a_1|^2\sigma_1 + \tilde{\sigma}_{\Lambda1}^{Z\gamma}/(\Lambda_1^{Z\gamma})^4 + \cdots}, \qquad \phi_{\Lambda1}^{Z\gamma}, \qquad (3)$$

where σ_i is the cross section for the process corresponding to $a_i = 1$ and all other couplings are set to zero. Since the production cross sections depend on the parton distribution functions (PDFs), the definition with respect to the decay process is more convenient. The cross section ratios defined in the $H \to 2e2\mu$ decay analysis [12] are adopted. Their values are $\sigma_1/\sigma_3 = 6.53$, $\sigma_1/\sigma_2 = 2.77$, $(\sigma_1/\tilde{\sigma}_{\Lambda1}) \times \text{TeV}^4 = 1.47 \times 10^4$, and $(\sigma_1/\tilde{\sigma}_{\Lambda1}^{Z\gamma}) \times \text{TeV}^4 = 5.80 \times 10^3$, as calculated using the JHUGEN7.0.2 event generator [26–29]. The ellipsis (…) in Eq. (3) indicates any other contribution not listed explicitly. Under the assumption that the couplings in Eq. (2) are constant and real, the above formulation is equivalent to an effective Lagrangian notation. Therefore, in this paper, the real coupling constants are tested, which means only $\phi_{ai} = 0$ or π are allowed. The constraints are set on the product $f_{ai}\cos(\phi_{ai})$, which ranges from -1 to $+1$.

Anomalous effects in the $H \to \tau\tau$ decay and $t\bar{t}H$ production are described by the Hff couplings of the H boson to fermions, with generally two couplings κ_f and $\tilde{\kappa}_f$, CP-even and CP-odd, respectively. Similarly, if the gluon coupling Hgg is dominated by the top quark loop, it can be described with the κ_t and $\tilde{\kappa}_t$ parameters. However, since other heavy states may contribute to the loop, we consider the effective Hgg coupling using the more general parametrization given in Eq. (2) instead of explicitly including the quark loop. In particular, the effective cross section fraction in gluon fusion becomes

$$f_{a3}^{ggH} = \frac{|a_3^{ggH}|^2}{|a_2^{ggH}|^2 + |a_3^{ggH}|^2}, \qquad (4)$$

where the cross sections $\sigma_2^{ggH} = \sigma_3^{ggH}$ drop out from the equation following the coupling convention in Eq. (2).

Experimentally observable effects resulting from the above anomalous couplings are discussed in the next section. In this paper, anomalous HWW, HZZ, and $HZ\gamma$ couplings are considered in VBF and VH production, and anomalous Hgg couplings are considered in gluon fusion. Since CP-violating effects in electroweak (VBF and VH) and gluon fusion production modify the same kinematic distributions, both CP-sensitive parameters, f_{a3} and f_{a3}^{ggH}, are left unconstrained simultaneously. It has been checked that CP violation in $H \rightarrow \tau\tau$ decays would not affect these measurements. Under the assumption that the couplings are constant and real, the above formulation is equivalent to an effective Lagrangian notation. Therefore, in this paper, the real coupling constants are tested, and results are presented for the product of f_{ai} and $\cos(\phi_{ai})$, the latter being the sign of the real ratio of couplings a_i/a_1.

Following the formalism discussed in this section, simulated samples of H boson events produced via anomalous HVV couplings (VBF, VH, gluon fusion in association with two jets) are generated using JHUGEN. The associated production in gluon fusion with two jets is affected by anomalous interactions, while the kinematics of the production with zero or one jet are not affected. The latter events are generated with POWHEG2.0 [52–55], which is used for yield normalization of events selected with two jets and for the description of event distributions in categories of events where the correlation of the two jets is not important. For the kinematics relevant to this analysis in VBF and VH production, the effects that appear at next-to-leading order (NLO) in QCD are well approximated by the leading-order (LO) QCD matrix elements used in JHUGEN, combined with parton showering. The JHUGEN samples produced with the SM couplings are compared with the equivalent samples generated by the POWHEG event generator at NLO QCD, with parton showering applied in both cases, and the kinematic distributions are found to agree.

The PYTHIA8.212 [56] event generator is used to model the H boson decay to τ leptons and the decays of the τ leptons. Both scalar and pseudoscalar $H \rightarrow \tau\tau$ decays and their interference have been modeled to confirm that the analysis does not depend on the decay model. The default samples are generated with the scalar hypothesis in decay. The PDFs used in the generators are NNPDF30 [57], with their precision matching that of the matrix elements. All MC samples are further processed through a dedicated simulation of the CMS detector based on GEANT4 [58].

To simulate processes with anomalous H boson couplings, for each type of anomalous coupling, we generate events with both the pure anomalous term and its interference with the SM contribution in the production HVV interaction. This allows extraction of the various coupling components and their interference. The MELA package, based on JHUGEN matrix elements, permits the application of weights to events in any sample to model any other HVV or Hff couplings with the same production mechanism. Reweighting enables one to increase the effective simulated event count by using all samples at once to describe any model, even if it has not been simulated. The MELA package also allows calculation of optimal discriminants for further analysis, as discussed in Sec. V.

Simulated samples for the modeling of background processes and of the H boson signal processes with SM couplings are the same as those used for the observation of the H boson decay to a pair of τ leptons [24]. All the corrections applied to samples are the same as in Ref. [24]. The MG5_aMC@NLO [59] generator is used for $Z +$ jets and $W +$ jets processes. They are simulated at LO with the MLM jet matching and merging [60]. The MG5_aMC@NLO generator is also used for diboson production simulated at NLO with the FxFx jet matching and merging [61], whereas POWHEG versions 2.0 and 1.0 are used for $t\bar{t}$ and single top quark production, respectively. The generators are interfaced with PYTHIA to model the parton showering and fragmentation. The PYTHIA parameters affecting the description of the underlying event are set to the CUETP8M1 tune [62].

V. DISCRIMINANT DISTRIBUTIONS

The full kinematic information for both production and decay of the H boson can be extracted from each event. This paper focuses on the production process, illustrated in Fig. 2. The techniques discussed below are similar to those used in earlier analyses by CMS, such as in Ref. [17].

Sensitivity to quantum numbers and anomalous couplings of the H boson is provided by the angular correlations between the two jets, the H boson, and the beam line direction in VBF, VH, or gluon fusion production with an additional two jets. A set of observables could be defined in VBF or VH production, such as $\vec{\Omega} = \{\theta_1, \theta_2, \Phi, \theta^*, \Phi_1, q_1^2, q_2^2\}$ for the VBF or VH process with the angles illustrated in Fig. 2 and the q_1^2 and q_2^2 discussed in reference to Eq. (2), as described in detail in Ref. [28]. It is, however, a challenging task to perform an optimal analysis in a multidimensional space of observables. The MELA is designed to reduce the number of observables to the minimum while retaining all essential information for the purpose of a particular measurement. In this analysis, the background suppression is still provided by the observables defined in Ref. [24].

When the H boson and two associated jets are reconstructed, two types of discriminants can be used to optimally search for anomalous couplings. These two discriminants rely only on signal matrix elements and are well defined. One can apply the Neyman-Pearson lemma [63] to prove that the two discriminants constitute a minimal and complete set of optimal observables [28,29] for the measurement of the f_{ai} parameter. One type of discriminant is designed to separate the process with
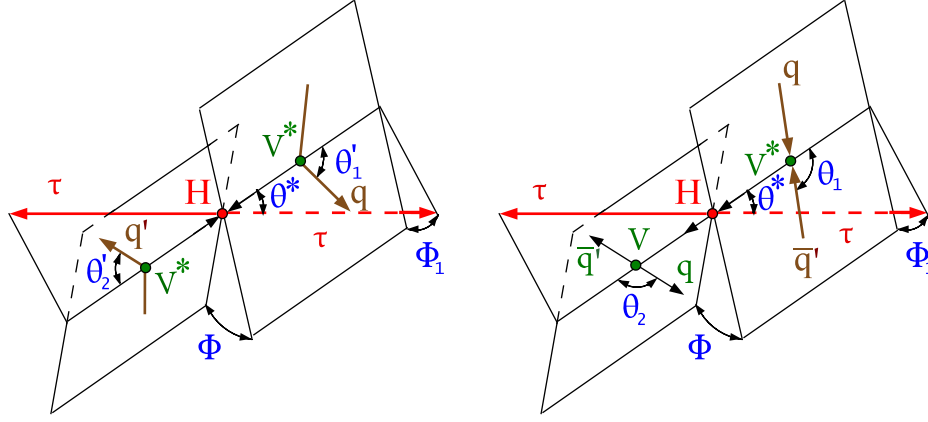
FIG. 2.   Illustrations of H boson production in $qq' \to gg(qq') \to H(qq') \to \tau\tau(qq')$ or VBF $qq' \to V^*V^*(qq') \to H(qq') \to \tau\tau(qq')$ (left) and in associated production $q\bar{q}' \to V^* \to VH \to q\bar{q}'\tau\tau$ (right). The $H \to \tau\tau$ decay is shown without further illustrating the τ decay chain. Angles and invariant masses fully characterize the orientation of the production and two-body decay chain and are defined in suitable rest frames of the V and H bosons, except in the VBF case, where only the H boson rest frame is used [26,28].

anomalous couplings, denoted as BSM, from the SM signal process,

$$\mathcal{D}_{\mathrm{BSM}} = \frac{\mathcal{P}_{\mathrm{SM}}(\vec{\Omega})}{\mathcal{P}_{\mathrm{SM}}(\vec{\Omega}) + \mathcal{P}_{\mathrm{BSM}}(\vec{\Omega})}, \qquad (5)$$

where $\mathcal{P}$ is the probability for the signal VBF production process (either SM or BSM), calculated using the matrix element MELA package and is normalized so that the matrix elements give the same cross sections for either $f_{ai} = 0$ or 1 in the relevant phase space of each process. Such a normalization leads to an optimal population of events in the range between 0 and 1. The discriminants are denoted as $\mathcal{D}_{0-}$, $\mathcal{D}_{0h+}$, $\mathcal{D}_{\Lambda 1}$, or $\mathcal{D}_{\Lambda 1}^{Z\gamma}$, depending on the targeted anomalous coupling a_3, a_2, Λ_1, or $\Lambda_1^{Z\gamma}$, respectively.

The second type of discriminant targets the contribution from interference between the SM and BSM processes,

$$\mathcal{D}_{\mathrm{int}} = \frac{\mathcal{P}_{\mathrm{SM-BSM}}^{\mathrm{int}}(\vec{\Omega})}{\mathcal{P}_{\mathrm{SM}}(\vec{\Omega}) + \mathcal{P}_{\mathrm{BSM}}(\vec{\Omega})}, \qquad (6)$$

where $\mathcal{P}_{\mathrm{SM-BSM}}^{\mathrm{int}}$ is the probability distribution for interference of SM and BSM signals in VBF production. This discriminant is used only for the CP-odd amplitude analysis with f_{a3} and is denoted $\mathcal{D}_{CP}$ in the rest of the paper. In the cases of $f_{\Lambda 1}$ and $f_{\Lambda 1}^{Z\gamma}$, the interference discriminants do not carry additional information because of their high correlation with the $\mathcal{D}_{\Lambda 1}$ and $\mathcal{D}_{\Lambda 1}^{Z\gamma}$ discriminants. The f_{a2} interference discriminant is not used in this analysis either, as it only becomes important for measurements of smaller couplings than presently tested and because of the limited number of events available for background parametrization.

Kinematic distributions of associated particles in gluon fusion are also sensitive to the quantum numbers of the H boson and to anomalous Hgg couplings. A set of observables, $\vec{\Omega}$, identical to those from the VBF process also describes this process. In this analysis, the focus is on the VBF-enhanced phase space in which the selection efficiency for the gluon fusion process is relatively small. Furthermore, the observables defined in Eqs. (5) and (6) for the VBF process are found to provide smaller separation between CP-even and CP-odd H boson couplings for gluon fusion production than MELA discriminants that would be dedicated to the gluon fusion process. Nonetheless, both parameters sensitive to CP violation, f_{a3} and f_{a3}^{ggH}, are included in a simultaneous fit using the observables optimized for the VBF process to avoid any possible bias in the measurement of f_{a3}.

While the correlations between the two jets, the H boson, and the beam line provide primary information about CP violation and anomalous couplings in electroweak production (VBF and VH), even events with reduced kinematic information can facilitate this analysis. For example, in cases where both jets lie outside of the detector acceptance, the p_{T} distribution of the H boson is different for SM and BSM production. This leads to different event populations across the three categories and to a different p_{T} distribution of the H boson in the boosted category. For example, the fraction of signal events is much smaller in the 0-jet category, and the p_{T} distribution is significantly harder in the boosted category for pseudoscalar H boson production than it is for the SM case. These effects are illustrated in Figs. 3–5. The same effects are, however, negligible in gluon fusion production, where both scalar and pseudoscalar Hgg couplings are generated by higher-dimension operators, which correspond to the a_2^{gg} and a_3^{gg} terms in Eq. (2).

Other observables, such as $\Delta\Phi_{JJ}$ [43], defined as the azimuthal difference between the two associated jets, have been suggested for the study of *CP* effects. While they do provide sensitivity to *CP* measurements, they are not as sensitive as the discriminant variables for VBF production used in this analysis. Nonetheless, as an alternative to the optimal VBF analysis with the MELA discriminants, we also performed a cross-check analysis where the $\Delta\Phi_{JJ}$ observable is used instead. It was verified that the expected precision on f_{a3} is indeed lower than in the optimal VBF analysis. On the other hand, the sensitivity of the $\Delta\Phi_{JJ}$ observable to the f_{a3}^{ggH} parameter is better than that of the VBF discriminants, and it is close to but not as good as the optimal MELA observables targeting the gluon fusion topology in association with two jets. Both results are discussed in Sec. VII.

VI. ANALYSIS IMPLEMENTATION

Five anomalous HVV coupling parameters defined in Sec. IV are studied: f_{a3}, f_{a2}, $f_{\Lambda1}$, $f_{\Lambda1}^{Z\gamma}$, and f_{a3}^{ggH} describing anomalous couplings in VBF, VH, and gluon fusion production. The *CP*-sensitive parameters f_{a3} and f_{a3}^{ggH} are studied jointly, while all other parameters are examined independently. Anomalous H boson couplings in other production mechanisms and in the $H \to \tau\tau$ decay do not affect these measurements, as the distributions studied here are insensitive to such effects.

The data, represented by a set of observables $\vec{x}$, are used to set constraints on anomalous coupling parameters. In the case of the *CP* study, the coupling parameters are f_{a3} and ϕ_{a3}. We also consider the scalar anomalous couplings described by f_{a2} and ϕ_{a2}, $f_{\Lambda1}$ and $\phi_{\Lambda1}$, and $f_{\Lambda1}^{Z\gamma}$ and $\phi_{\Lambda1}^{Z\gamma}$.

Since only real couplings are considered, we fit for the products $f_{a3}\cos(\phi_{a3})$ with $\cos(\phi_{a3}) = \pm1$, $f_{a2}\cos(\phi_{a2})$ with $\cos(\phi_{a2}) = \pm1$, $f_{\Lambda1}\cos(\phi_{\Lambda1})$ with $\cos(\phi_{\Lambda1}) = \pm1$, and $f_{\Lambda1}^{Z\gamma}\cos(\phi_{\Lambda1}^{Z\gamma})$ with $\cos(\phi_{\Lambda1}^{Z\gamma}) = \pm1$.

A. Observable distributions

Each event is described by its category k and the corresponding observables $\vec{x}$. In the 0-jet and boosted categories, which are dominated by the gluon fusion production mechanism, the observables are identical to those used in Ref. [24], namely $\vec{x} = \{m_{\text{vis}}, M\}$ in the $e\tau_{\text{h}}$ and $\mu\tau_{\text{h}}$ 0-jet categories, $\vec{x} = \{m_{\text{vis}}, p_{\text{T}}^{\mu}\}$ in the $e\mu$0-jet category, $\vec{x} = \{m_{\tau\tau}\}$ in the 0-jet $\tau_{\text{h}}\tau_{\text{h}}$ category, and $\vec{x} = \{m_{\tau\tau}, p_{\text{T}}^{H}\}$ in the boosted categories, where M is the τ_{h} decay mode, p_{T}^{μ} is the transverse momentum of the muon, and p_{T}^{H} is the transverse momentum of the H boson. There are no dedicated observables sensitive to anomalous couplings in these categories, as it is not possible to construct them in the absence of a correlated jet pair. Nonetheless, distributions of events in the above observables and categories still differ between signal models with variation of anomalous couplings.

In Figs. 3 and 4, the distributions of m_{vis} and $m_{\tau\tau}$ are displayed for selected events in the 0-jet category, and the transverse momentum distribution of the H boson is shown for the boosted category. Anomalous couplings would result in higher transverse momentum of the H boson and, unlike SM production, would cause the events to preferentially populate the boosted category instead of the one with no jets in the final state. The observable $m_{\tau\tau}$ is used in the $\tau_{\text{h}}\tau_{\text{h}}$ decay channel and m_{vis} in other channels in the 0-jet category. Two observables are used in the likelihood fit in the boosted category, $m_{\tau\tau}$ and p_{T}^{H}.
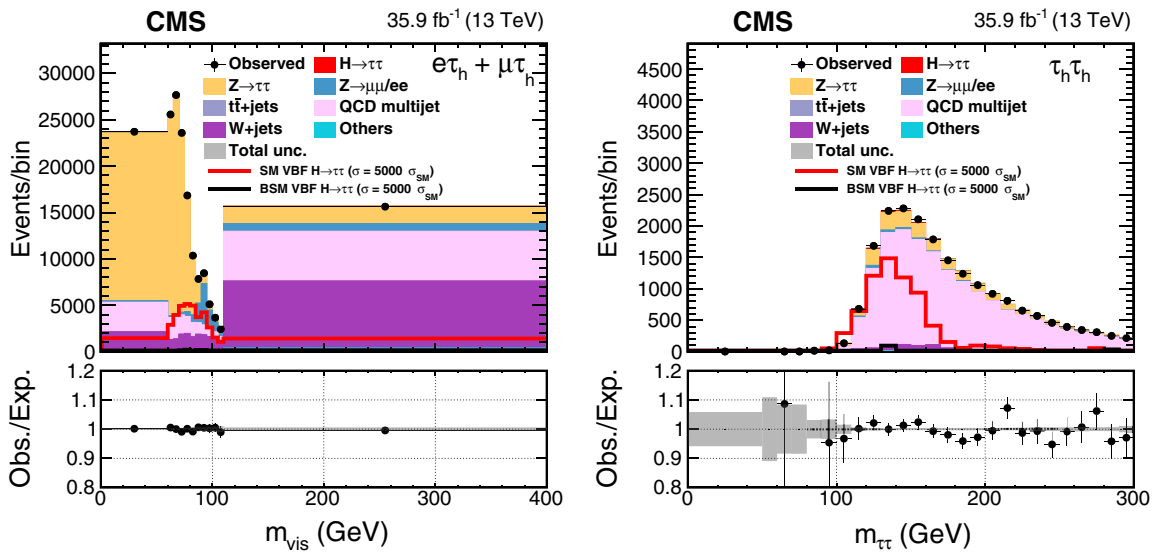

FIG. 3.   The distributions of m_{vis} and $m_{\tau\tau}$ in the 0-jet category of the $e\tau_{\text{h}} + \mu\tau_{\text{h}}$ (left) and $\tau_{\text{h}}\tau_{\text{h}}$ (right) decay channels. The BSM hypothesis corresponds to $f_{a3}\cos(\phi_{a3}) = 1$.
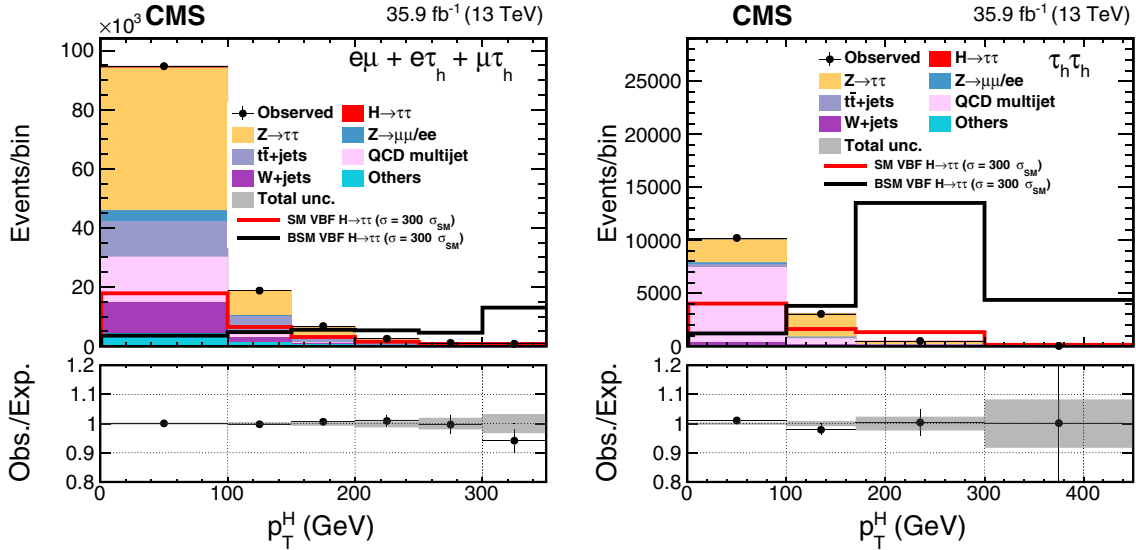
FIG. 4.　The distributions of transverse momentum of the H boson in the boosted category of the $e\tau_h + \mu\tau_h + e\mu$ (left) and $\tau_h\tau_h$ (right) decay channels. The BSM hypothesis corresponds to $f_{a3}\cos(\phi_{a3}) = 1$.

The contributions from BSM and SM yields in the boosted category are different in the $\tau_h\tau_h$ and $\ell\tau_h$ channels because of different trigger conditions and classification requirements. In Fig. 3, the contribution from the $e\mu$ channel is omitted because of its low sensitivity and different binning in the fit. The normalization of the predicted background distributions corresponds to the result of the likelihood fit described in Sec. VI B. In all production modes in Figs. 3 and 4, the $H \to \tau\tau$ process is normalized to its best-fit signal strength and couplings and is shown as an open overlaid histogram. The background components labeled in the figures as "others" include events from diboson and single top quark production, as well as H boson decays to W boson pairs. The uncertainty band accounts for all sources of uncertainty. The SM prediction for the VBF $H \to \tau\tau$ signal, multiplied by a factor 5000 (300) in Fig. 3 (4), is shown as a red open overlaid histogram. The black open overlaid histogram represents a BSM hypothesis for the VBF $H \to \tau\tau$ signal, normalized to 5000 (300) times the predicted SM cross section in Fig. 3 (4).

In Figs. 5–9, the discriminant distributions in the VBF category are displayed. In the VBF category, either three or four observables are used in the likelihood fit: $\vec{x} = \{m_{JJ}, m_{\tau\tau}, \mathcal{D}_{0-}, \mathcal{D}_{CP}\}$ are used to determine the f_{a3} parameter, $\vec{x} = \{m_{JJ}, m_{\tau\tau}, \mathcal{D}_{0h+}\}$ are used to determine the f_{a2} parameter, $\vec{x} = \{m_{JJ}, m_{\tau\tau}, \mathcal{D}_{\Lambda1}\}$ are used to determine the $f_{\Lambda1}$ parameter, and $\vec{x} = \{m_{JJ}, m_{\tau\tau}, \mathcal{D}_{\Lambda1}^{Z\gamma}\}$ are used to determine the $f_{\Lambda1}^{Z\gamma}$ parameter, as defined in Eqs. (5) and (6). In order to keep the background and signal templates sufficiently populated, a smaller number of bins is chosen for m_{JJ} and $m_{\tau\tau}$ compared to Ref. [24]. It was found that four bins in $\mathcal{D}_{0-}$, $\mathcal{D}_{0h+}$, $\mathcal{D}_{\Lambda1}$, and $\mathcal{D}_{\Lambda1}^{Z\gamma}$ are sufficient for close-to-optimal performance. At the same time, we adopt

two bins in $\mathcal{D}_{CP}$ with $\mathcal{D}_{CP} < 0$ and $\mathcal{D}_{CP} > 0$. This choice does not lead to the need for additional bins in the templates, because all distributions except the CP-violating interference component are symmetric in $\mathcal{D}_{CP}$, and this symmetry is enforced in the templates. A forward-backward asymmetry in $\mathcal{D}_{CP}$ would be a clear indication of CP-sensitive effects and is present only in the signal interference template.

B. Likelihood parametrization

We perform an unbinned extended maximum likelihood fit [64] to the events split into several categories according to the three production topologies and four tau-lepton pair final states using the RooFit toolkit [65,66]. The probability density functions for signal $\mathcal{P}_{\rm sig}^{j,k}(\vec{x})$ and background $\mathcal{P}_{\rm bkg}^{j,k}(\vec{x})$ are binned templates and are defined for each production mechanism j in each category k. Each event is characterized by the discrete category k and up to four observables $\vec{x}$, depending on the category. For the VBF, VH, or gluon fusion production mechanisms, the signal probability density function is defined as

$$\mathcal{P}_{\rm sig}^{j,k}(\vec{x}) = (1 - f_{ai})\mathcal{T}_{a1}^{j,k}(\vec{x}) + f_{ai}\mathcal{T}_{ai}^{j,k}(\vec{x})$$
$$+ \sqrt{f_{ai}(1 - f_{ai})}\mathcal{T}_{a1,ai}^{j,k}(\vec{x})\cos(\phi_{ai}), \quad (7)$$

where $\mathcal{T}_{ai}^{j,k}$ is the template probability of a pure anomalous coupling a_i term and $\mathcal{T}_{a1,ai}^{j,k}$ describes the interference between the anomalous coupling and SM term a_1, or SM term a_2^{ggH} in the case of gluon fusion. Here, f_{ai} stands for either f_{a3}, f_{a2}, $f_{\Lambda1}$, $f_{\Lambda1}^{Z\gamma}$, or f_{a3}^{ggH}. Each term in Eq. (7) is extracted from a dedicated simulation.
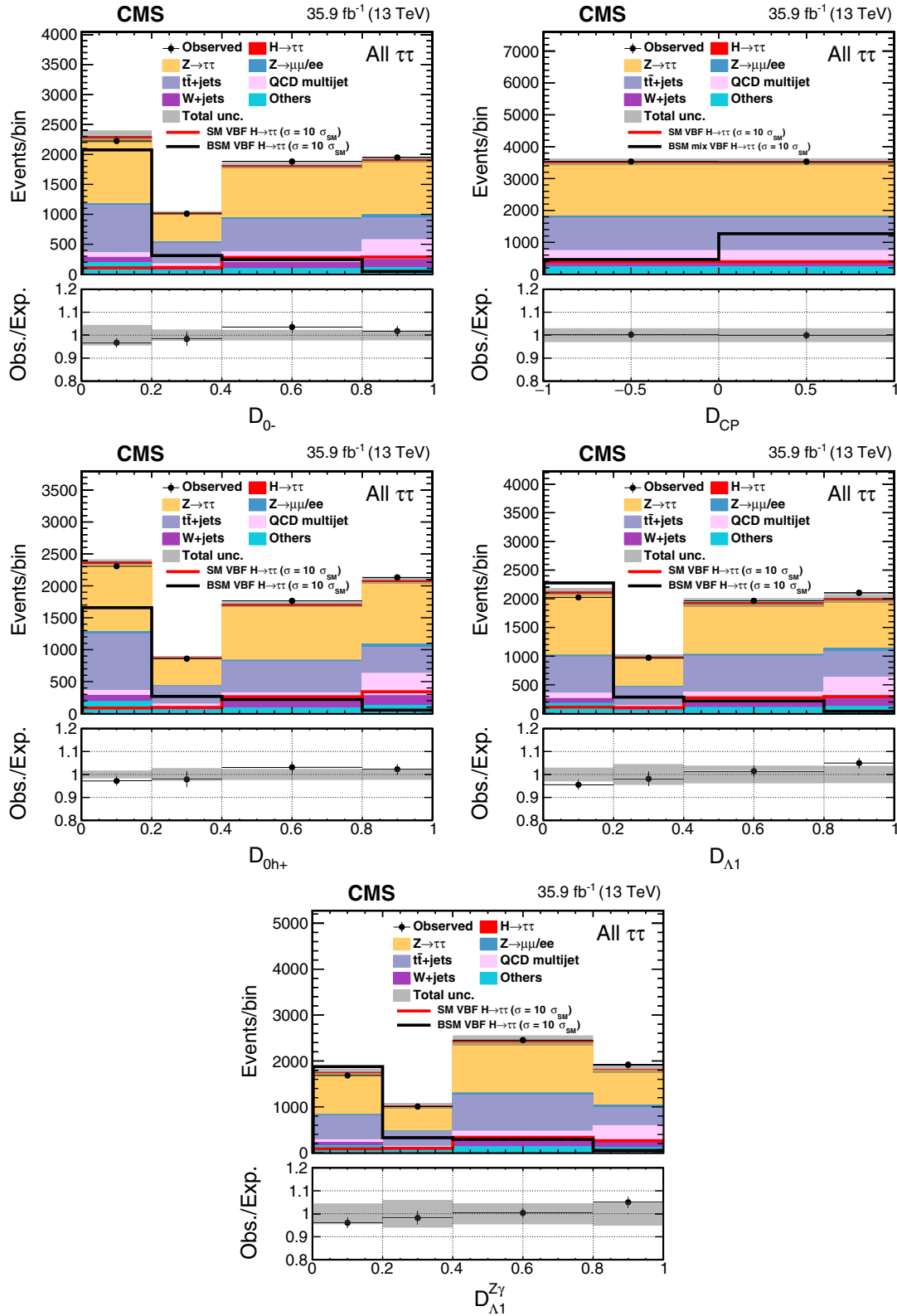
FIG. 5.   The distribution of $\mathcal{D}_{0-}$, $\mathcal{D}_{CP}$, $\mathcal{D}_{0h+}$, $\mathcal{D}_{\Lambda 1}$, and $\mathcal{D}_{\Lambda 1}^{Z\gamma}$ in the VBF category. All four decay channels, $e\mu$, $e\tau_{\mathrm{h}}$, $\mu\tau_{\mathrm{h}}$, and $\tau_{\mathrm{h}}\tau_{\mathrm{h}}$, are summed. The BSM hypothesis depends on the variable shown; it corresponds to $f_{a3}\cos(\phi_{a3}) = 1$ for the $\mathcal{D}_{0-}$ (upper left) distribution, the maximal mixing in VBF production ("BSM mix," corresponding to $f_{a3}\cos(\phi_{a3}) = 0.013$) for the $\mathcal{D}_{CP}$ distribution (upper right), $f_{a2}\cos(\phi_{a2}) = 1$ for the $\mathcal{D}_{0h+}$ distribution (middle left), $f_{\Lambda 1}\cos(\phi_{\Lambda 1}) = 1$ for the $\mathcal{D}_{\Lambda 1}$ distribution (middle right), and $f_{\Lambda 1}^{Z\gamma}\cos(\phi_{\Lambda 1}^{Z\gamma}) = 1$ for the $\mathcal{D}_{\Lambda 1}^{Z\gamma}$ distribution (lower). The expected $\mathcal{D}_{CP}$ distribution is always symmetric, unless a CP-violating effect is present in the signal.
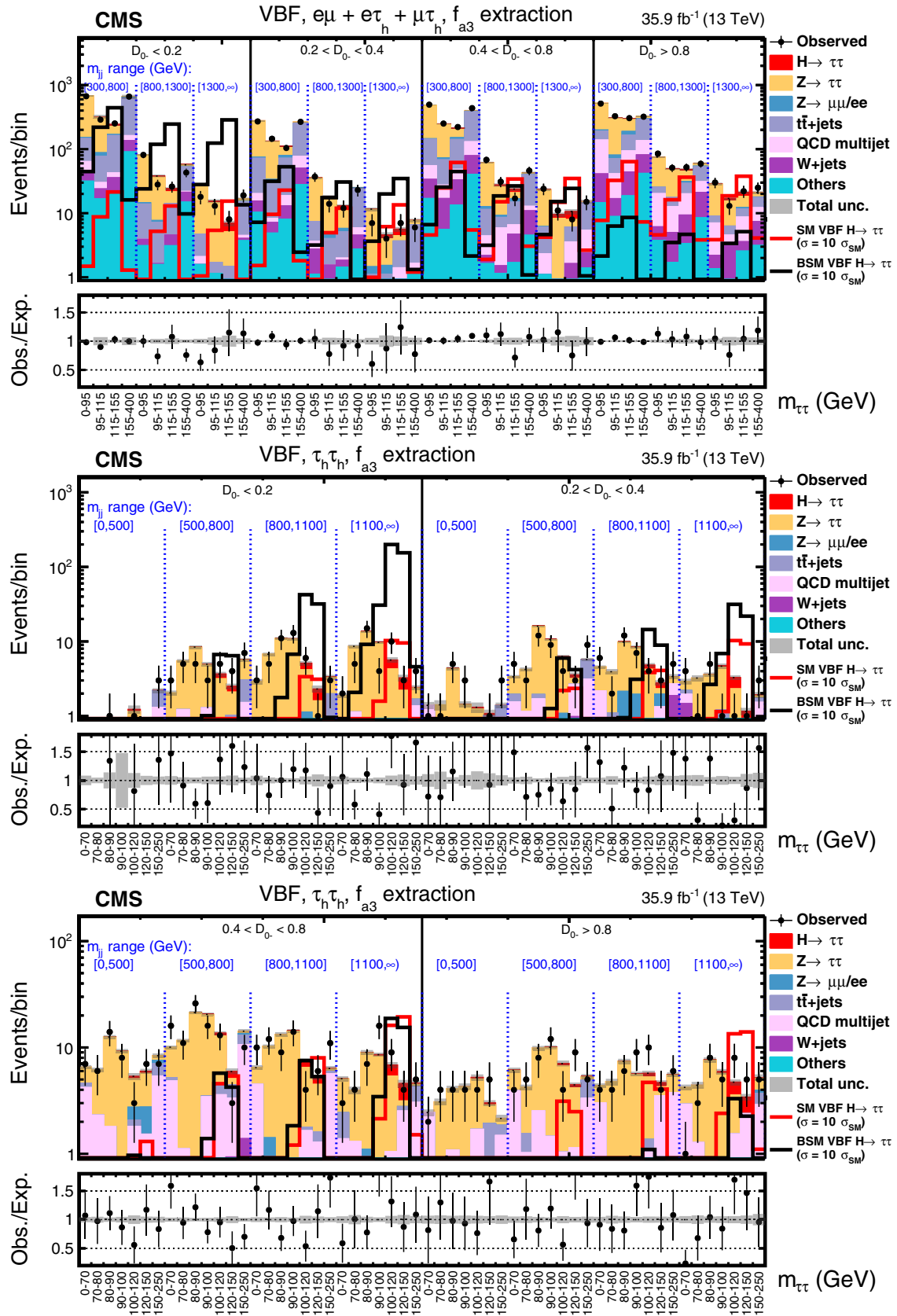
FIG. 6. Observed and expected distributions in the VBF category in bins of $m_{\tau\tau}$, m_{JJ}, and $\mathcal{D}_{0-}$ in the f_{a3} analysis for the $e\mu + e\tau_h + \mu\tau_h$ (upper) and $\tau_h\tau_h$ (middle and lower) decay channels.

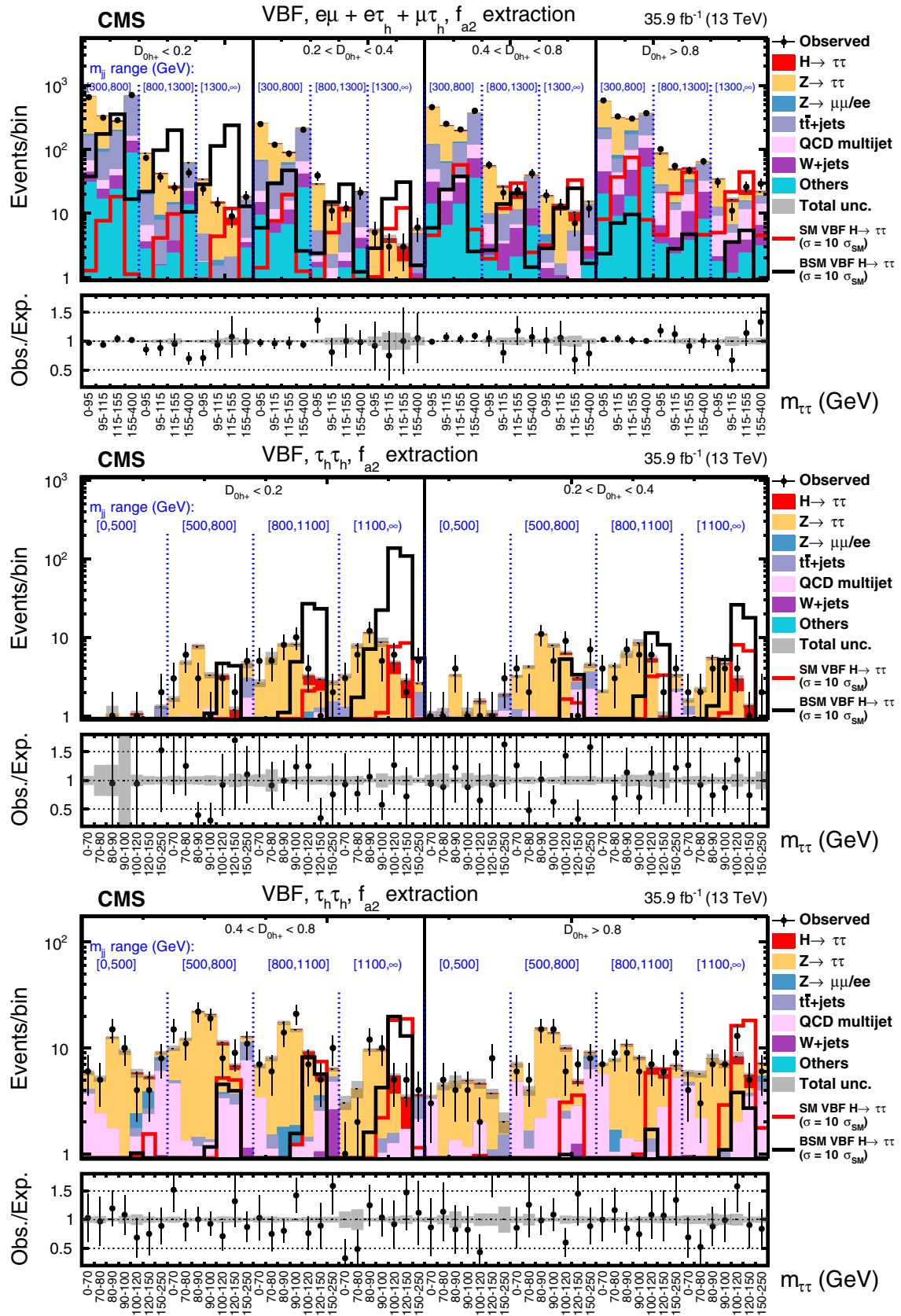FIG. 7.   Observed and expected distributions in the VBF category in bins of $m_{\tau\tau}$, m_{JJ}, and $\mathcal{D}_{0h+}$ in the f_{a2} analysis for the $e\mu + e\tau_h + \mu\tau_h$ (upper) and $\tau_h\tau_h$ (middle and lower) decay channels.
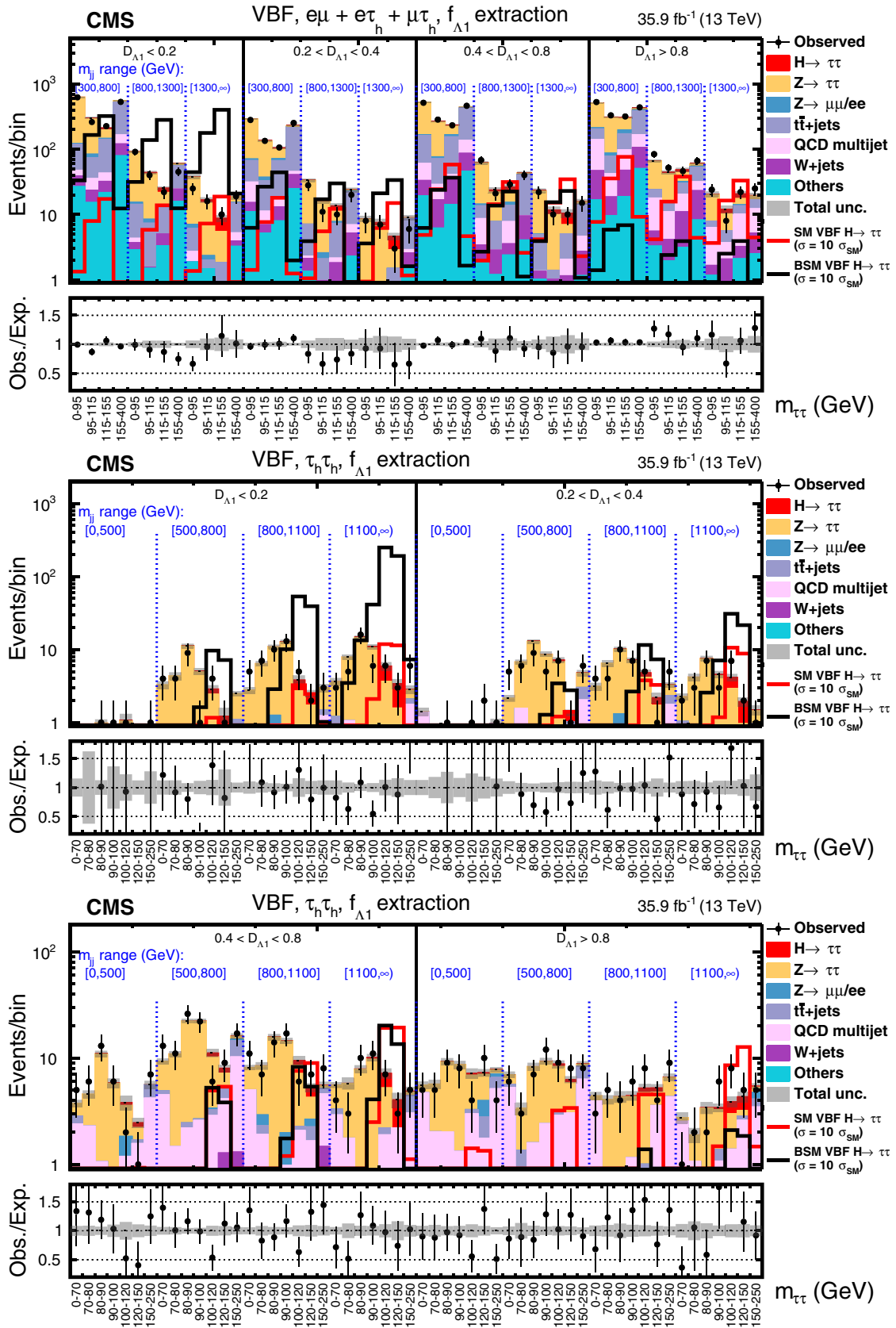
FIG. 8. Observed and expected distributions in the VBF category in bins of $m_{\tau\tau}$, m_{JJ}, and $\mathcal{D}_{\Lambda1}$ in the $f_{\Lambda1}$ analysis for the $e\mu + e\tau_h + \mu\mu$ (upper) and $\tau_h\tau_h$ (middle and lower) decay channels.
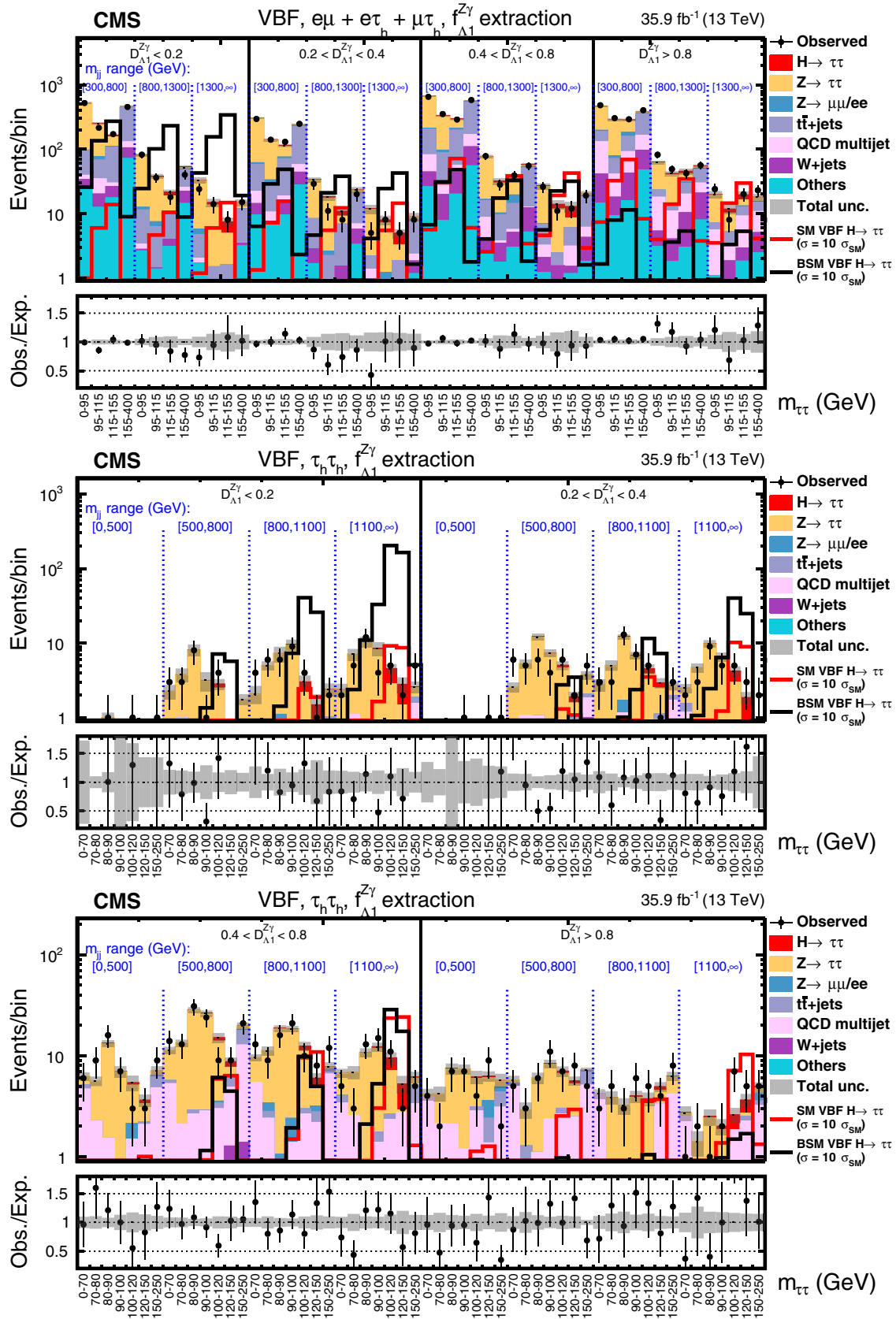
FIG. 9.   Observed and expected distributions in the VBF category in bins of $m_{\tau\tau}$, m_{JJ}, and $\mathcal{D}_{\Lambda 1}^{Z\gamma}$ in the $f_{\Lambda 1}^{Z\gamma}$ analysis for the $e\mu +$ $e\tau_h + \tau_h\tau_h$ (upper) and $\tau_h\tau_h$ (middle and lower) decay channels.

The signal strength parameters μ_V and μ_f are introduced as two parameters of interest. They scale the yields in the VBF $+ VH$ and gluon fusion production processes, respectively. They are defined such that for $f_{ai} = 0$ they are equal to the ratio of the measured to the expected cross sections for the full process, including the $H \to \tau\tau$ decay. The likelihood is maximized with respect to the anomalous coupling $f_{ai} \cos(\phi_{ai})$ and yield (μ_V, μ_f) parameters and with respect to the nuisance parameters, which include the constrained parameters describing the systematic uncertainties. The $f_{a3} \cos(\phi_{a3})$ and $f_{a3}^{ggH} \cos(\phi_{a3}^{ggH})$ parameters are tested simultaneously, while all other $f_{ai} \cos(\phi_{ai})$ parameters are tested independently. All parameters except the anomalous coupling parameter of interest $f_{ai} \cos(\phi_{ai})$ are profiled. The confidence level (C.L.) intervals are determined from profile likelihood scans of the respective parameters. The allowed 68 and 95% C.L. intervals are defined using the profile likelihood function, $-2\Delta \ln \mathcal{L} = 1.00$ and 3.84, respectively, for which exact coverage is expected in the asymptotic limit [67]. Approximate coverage has been tested with generated samples.

C. Systematic uncertainties

A log-normal probability density function is assumed for the nuisance parameters that affect the event yields of the various background and signal contributions, whereas systematic uncertainties that affect the distributions are represented by nuisance parameters of which the variation results in a continuous perturbation of the spectrum [68] and which are assumed to have a Gaussian probability density function. The systematic uncertainties are identical to those detailed in Ref. [24]. They are summarized in the following.

The rate uncertainties in the identification, isolation, and trigger efficiencies of electrons and muons amount to 2%. For τ_h, the uncertainty in the identification is 5% per τ_h candidate, and the uncertainty related to the trigger amounts to an additional 5% per τ_h candidate [39]. In the 0-jet category, where one of the dimensions of the two-dimensional fit is the reconstructed τ_h decay mode, the relative reconstruction efficiency in a given τ_h reconstructed decay mode has an uncertainty of 3% [24]. For muons and electrons misreconstructed as τ_h candidates, the τ_h identification leads to rate uncertainties of 25% and 12%, respectively [39]. This leads to the corresponding uncertainty in the rates of the $Z \to \mu\mu$ and $Z \to ee$ backgrounds misidentified as the $\mu\tau_h$ and $e\tau_h$ final states, respectively. The requirement that there are no b-tagged jets in $e\mu$ decay channel events results in a rate uncertainty as large as 5% in the $t\bar{t}$ background [69].

The uncertainties in the energy scales of electrons and τ_h leptons amount to 1.0%–2.5% and 1.2% [24,39], while the effect of the uncertainty in the muon energy scale is negligible. This uncertainty increases to 3.0% and 1.5%, respectively, for electrons and muons misidentified as τ_h

candidates [24]. For events where quark- or gluon-initiated jets are misidentified as τ_h candidates, a linear uncertainty that increases by 20% per 100 GeV in transverse momentum of the τ_h and amounts to 20% for a τ_h with p_T of 100 GeV is taken into account [24]. This uncertainty affects simulated events with jets misidentified as τ_h candidates, from various processes like the Drell-Yan, $t\bar{t}$, diboson, and $W +$ jets productions. Uncertainties in the jet and p_T^{miss} energy scales are determined event by event [70], and propagated to the observables used in the analysis.

The uncertainty in the integrated luminosity is 2.5% [71]. Per bin uncertainties in the template probability parametrization related to the finite number of simulated events, or to the limited number of events in data control regions, are also taken into account [68].

The rate and acceptance uncertainties for the signal processes related to the theoretical calculations are due to uncertainties in the PDFs, variations of the renormalization and factorization scales, and uncertainties in the modeling of parton showers. The magnitude of the rate uncertainty depends on the production process and on the event category. In particular, the inclusive uncertainty related to the PDFs amounts to 2.1% for the VBF production mode [72], while the corresponding uncertainty for the variation of the renormalization and factorization scales is 0.4% [72]. The acceptance uncertainties related to the particular selection criteria used in this analysis are less than 1% for all production modes. The theoretical uncertainty in the branching fraction of the H boson to τ leptons is 2.1% [72].

An overall rate uncertainty of 3%–10% affects the $Z \to \tau\tau$ background, depending on the category, as estimated from a control region enriched in $Z \to \mu\mu$ events. In the VBF category, this process is also affected by a shape uncertainty that depends on m_{JJ} and $\Delta\Phi_{JJ}$ and can reach a magnitude of 20%. In addition to the uncertainties related to the $W +$ jets control regions in the $e\tau_h$ and $\mu\tau_h$ final states, the $W +$ jets background is affected by a rate uncertainty ranging between 5% and 10% to account for the extrapolation of the constraints from the high-m_T to the low-m_T regions. In the $e\mu$ and $\tau_h\tau_h$ final states, the rate uncertainties in the $W +$ jets background yields are 20% and 4%, respectively.

The uncertainty in the QCD multijet background yield in the $e\mu$ decay channel ranges from 10% to 20%, depending on the category. In the $e\tau_h$ and $\mu\tau_h$ decay channels, uncertainties derived from the control regions are considered for the QCD multijet background, together with an additional 20% uncertainty that accounts for the extrapolation from the relaxed-isolation control region to the isolated signal region. In the $\tau_h\tau_h$ decay channel, the uncertainty in the QCD multijet background yield is a combination of the uncertainties obtained from fitting the dedicated control regions with τ_h candidates passing relaxed isolation criteria, of the extrapolation to the signal
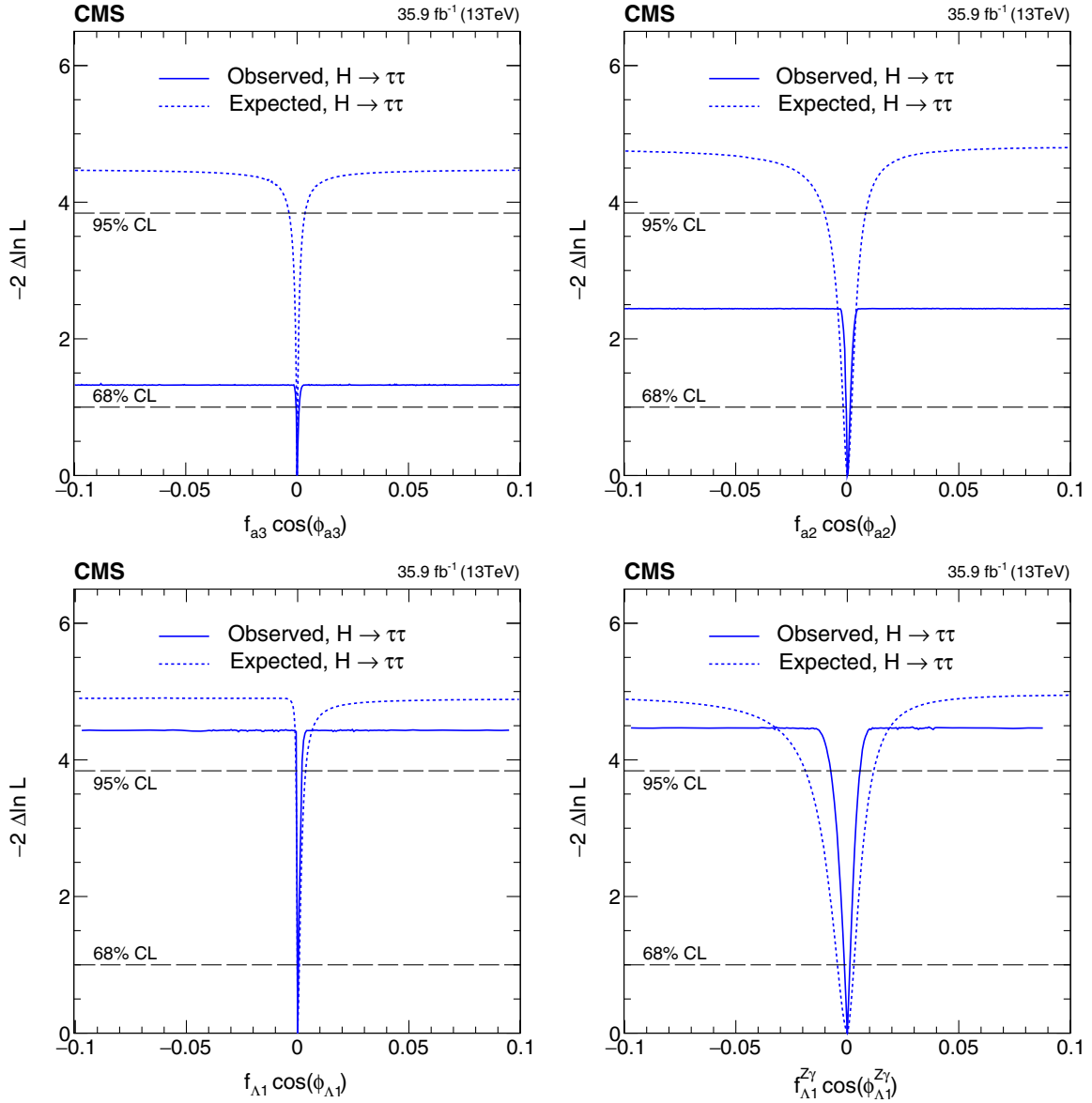
FIG. 10. Observed (solid) and expected (dashed) likelihood scans of $f_{a3}\cos(\phi_{a3})$ (top left), $f_{a2}\cos(\phi_{a2})$ (top right), $f_{\Lambda1}\cos(\phi_{\Lambda1})$ (bottom left), and $f_{\Lambda1}^{Z\gamma}\cos(\phi_{\Lambda1}^{Z\gamma})$ (bottom right).

region ranging from 3% to 15%, and of residual differences between prediction and data in signal-free regions with various loose isolation criteria.

The uncertainty from the fit in the $t\bar{t}$ control region results in an uncertainty of about 5% on the $t\bar{t}$ cross section in the signal region. The combined systematic uncertainty in the background yield arising from diboson and single top quark production processes is taken to be 5% [73,74].

The additional $\mathcal{D}_{0-}$, $\mathcal{D}_{0h+}$, $\mathcal{D}_{\Lambda1}$, and $\mathcal{D}_{\Lambda1}^{Z\gamma}$ observables do not change the procedure for estimating the systematic uncertainty, as any mismodeling due to detector effects is estimated with the same procedure as for any other distribution. None of the systematic uncertainties

TABLE II. Allowed 68% C.L. (central values with uncertainties) and 95% C.L. (in square brackets) intervals on anomalous coupling parameters using the $H \to \tau\tau$ decay. The observed 95% C.L. constraints on $f_{a3}\cos(\phi_{a3})$ and $f_{a2}\cos(\phi_{a2})$ allow the full range $[-1, 1]$.

	Observed/(10^{-3})		Expected/(10^{-3})	
Parameter	68% C.L.	95% C.L.	68% C.L.	95% C.L.
$f_{a3}\cos(\phi_{a3})$	$0.00^{+0.93}_{-0.43}$	$\cdots$	0.00 ± 0.28	$[-3.6, 3.6]$
$f_{a2}\cos(\phi_{a2})$	$0.0^{+1.2}_{-0.4}$	$\cdots$	$0.0^{+2.0}_{-1.8}$	$[-10.0, 8.0]$
$f_{\Lambda1}\cos(\phi_{\Lambda1})$	$0.00^{+0.39}_{-0.10}$	$[-0.4, 1.8]$	$0.00^{+0.75}_{-0.16}$	$[-0.8, 3.6]$
$f_{\Lambda1}^{Z\gamma}\cos(\phi_{\Lambda1}^{Z\gamma})$	$0.0^{+1.2}_{-1.3}$	$[-7.4, 5.6]$	$0.0^{+3.0}_{-4.5}$	$[-19, 12]$

introduces asymmetry in the $\mathcal{D}_{CP}$ distributions which remain symmetric, except for the antisymmetric signal interference contribution.

VII. RESULTS

The four sets of f_{ai} and ϕ_{ai} parameters describing anomalous *HVV* couplings, as defined in Eqs. (2) and (3), are tested against the data according to the probability density defined in Eq. (7). The results of the likelihood scans are shown in Fig. 10 and listed in Table II. In each fit,

the values of the other anomalous coupling parameters are set to zero. In the case of the *CP* fit, the f_{a3} parameter is measured simultaneously with f_{a3}^{ggH}, as defined in Eq. (4). All other parameters, including the signal strength parameters μ_V and μ_f, are profiled. The results are presented for the product of f_{ai} and $\cos(\phi_{ai})$, the latter being the sign of the real a_i/a_1 ratio of couplings. In this approach, the f_{ai} parameter is constrained to be in the physical range $f_{ai} \geq 0$. Therefore, in the SM, it is likely for the best-fit value to be at the physical boundary $f_{ai} = 0$ for both signs of the a_i/a_1 ratio.
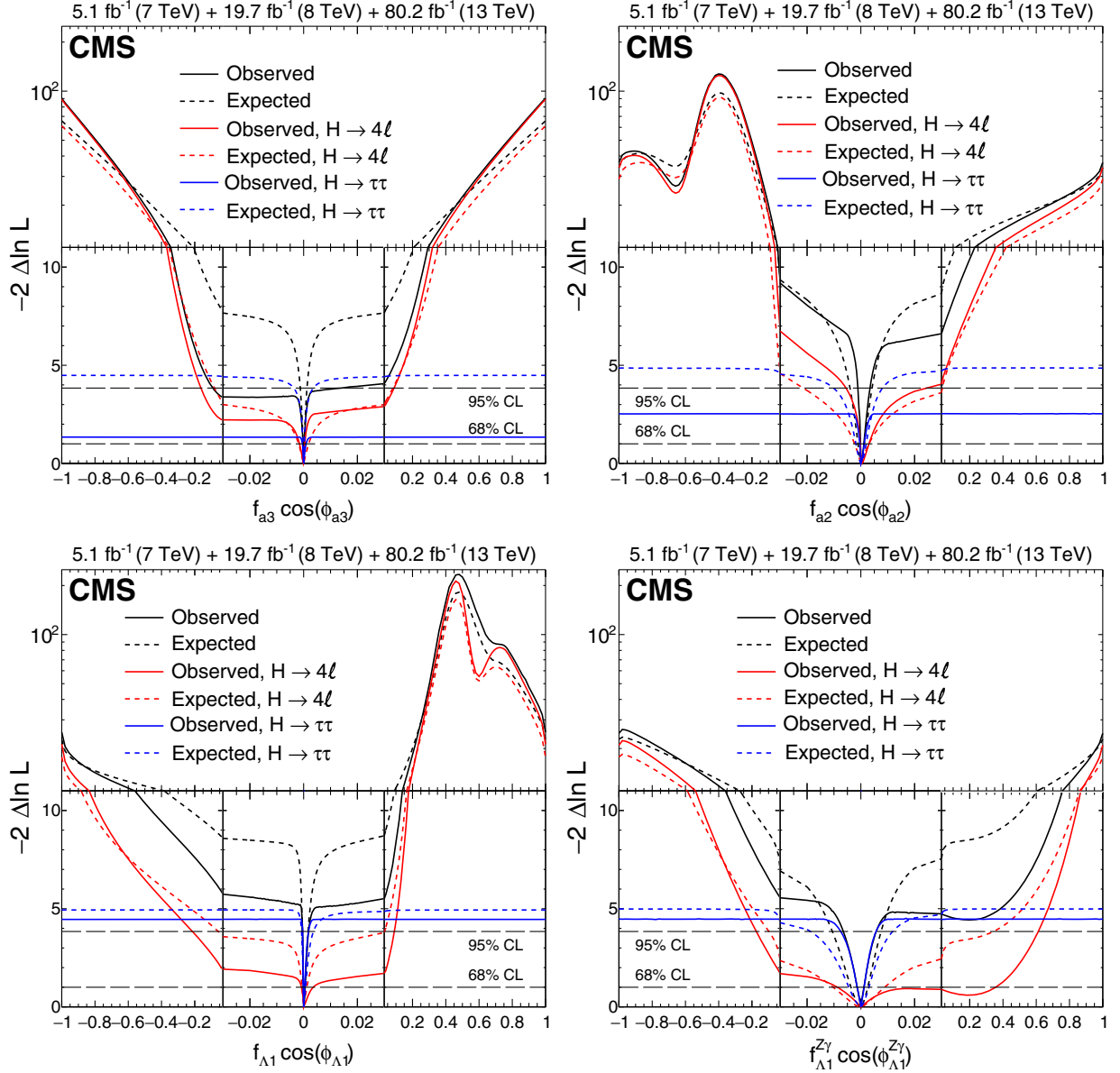

FIG. 11. Combination of results using the $H \to \tau\tau$ decay (presented in this paper) and the $H \to 4\ell$ decay [17]. The observed (solid) and expected (dashed) likelihood scans of $f_{a3}\cos(\phi_{a3})$ (top left), $f_{a2}\cos(\phi_{a2})$ (top right), $f_{\Lambda 1}\cos(\phi_{\Lambda 1})$ (bottom left), and $f_{\Lambda 1}^{Z\gamma}\cos(\phi_{\Lambda 1}^{Z\gamma})$ (bottom right) are shown. For better visibility of all features, the x and y axes are presented with variable scales. On the linear-scale x axis, a zoom is applied in the range -0.03 to 0.03. The y axis is shown in linear (logarithmic) scale for values of $-2\Delta \ln \mathcal{L}$ below (above) 11.

The constraints on $f_{ai} \cos(\phi_{ai})$ appear relatively tight compared to similar constraints utilizing the H boson decay information, e.g., in Ref. [17]. This is because the cross section in VBF and VH production increases quickly with f_{ai}. The definition of f_{ai} in Eq. (3) uses the cross section ratios defined in the $H \to 2e2\mu$ decay as the common convention across various measurements. Because the cross section increases with respect to f_{ai} at different rates for production and decay, relatively small values of f_{ai} correspond to a substantial anomalous contribution to the production cross section. This leads to the plateau in the $-2\ln(\mathcal{L}/\mathcal{L}_{\max})$ distributions for larger values of $f_{ai} \cos(\phi_{ai})$ in Fig. 10. If we had used the cross section ratios for VBF production in the f_{ai} definition in Eq. (3), the appearance of the plateau and the narrow exclusion range would change. For example, the 68% C.L. upper constraint on $f_{a3} \cos(\phi_{a3}) < 0.00093$ is dominated by the VBF production information. If we were to use the VBF cross section ratio $\sigma_1^{\mathrm{VBF}}/\sigma_3^{\mathrm{VBF}} = 0.089$ in the f_{a3}^{VBF} definition in Eq. (3), this would correspond to the upper constraint $f_{a3}^{\mathrm{VBF}} \cos(\phi_{a3}) < 0.064$ at 68% C.L.

The observed maximum value of $-2\ln(\mathcal{L}/\mathcal{L}_{\max})$ is somewhat different from expectation and between the four analyses, mostly due to statistical fluctuations in the distribution of events across the dedicated discriminants and other observables, leading to different significances of the observed signal driven by VBF and VH production. In particular, the best-fit values for (μ_V, μ_f) in the four analyses, under the assumption that $f_{ai} = 0$, are $(0.55 \pm 0.48, 1.03^{+0.45}_{-0.40})$ at $f_{a3} = 0$, $(0.72^{+0.48}_{-0.46}, 0.89^{+0.43}_{-0.37})$ at $f_{a2} = 0$, $(0.92^{+0.44}_{-0.45}, 0.82^{+0.46}_{-0.38})$ at $f_{\Lambda 1} = 0$, and $(0.94^{+0.48}_{-0.46}, 0.79 \pm 0.40)$ at $f_{\Lambda 1}^{Z\gamma} = 0$. This results in a somewhat lower yield of VBF and VH events observed in the first two cases, leading to lower confidence levels in constraints on $f_{a3} \cos(\phi_{a3})$ and $f_{a2} \cos(\phi_{a2})$.

In the f_{a3} analysis, a simultaneous measurement of f_{a3} and f_{a3}^{ggH} is performed. These are the parameters sensitive to CP in the VBF and gluon fusion processes, respectively. Both the observed and expected exclusions from the null hypothesis for any BSM gluon fusion scenario with either MELA or the $\Delta\Phi_{JJ}$ observable are below one standard deviation.

VIII. COMBINATION OF RESULTS WITH OTHER CHANNELS

The precision of the coupling measurements can be improved by combining the results in the $H \to \tau\tau$ channel, presented here, with those of other H boson decay channels. A combination is possible only with those channels where anomalous couplings in the VH, VBF, and gluon fusion processes are taken into account in the fit in a consistent way. If it is not done, the kinematics of the associated jets and of the H boson would not be

modeled correctly for BSM values of the f_{ai} or f_{a3}^{ggH} parameters.

In the example of the CP fit, in the stand-alone fit with the $H \to \tau\tau$ channel, the parameters of interest are $f_{a3} \cos(\phi_{a3})$, $f_{a3}^{ggH} \cos(\phi_{a3}^{ggH})$, $\mu_V^{H\tau\tau}$, and $\mu_f^{H\tau\tau}$. When reporting one parameter, all other parameters are profiled. In a combined fit of the $H \to \tau\tau$ and $H \to VV$ channels, such as in Ref. [17], in principle there are four signal strength parameters in the two channels ($\mu_V^{H\tau\tau}$, $\mu_f^{H\tau\tau}$, μ_V^{HVV}, μ_f^{HVV}). However, this can be reduced to three parameters because the ratio between the VBF $+ VH$ and gluon fusion cross sections is expected to be the same in each of the two channels, that is $\mu_V^{H\tau\tau}/\mu_f^{H\tau\tau} = \mu_V^{HVV}/\mu_f^{HVV}$. Therefore, the three signal strength parameters are chosen as μ_V, μ_f, and η_τ, where the last one is the relative strength of the H boson coupling to the τ leptons. We should note that, as discussed earlier, the HWW couplings are analyzed together with the HZZ couplings assuming $a_i^{ZZ} = a_i^{WW}$. The results can be reinterpreted for a different assumption of the a_i^{ZZ}/a_i^{WW} ratio [17]. In the combined likelihood fit, all common systematic uncertainties are correlated between the channels, both theoretical uncertainties, such as those due to the PDFs, and experimental uncertainties, such as jet energy calibration.

The results using the $H \to \tau\tau$ decay are combined with those presented in Ref. [17] using the on-shell $H \to 4\ell$ decay. The latter employs results from Run 1 (from 2011 and 2012) and Run 2 (from 2015, 2016, and 2017) with data corresponding to integrated luminosities of 5.1, 19.7, and 80.2 fb^{-1} at center-of-mass energies 7, 8, and 13 TeV, respectively. In this analysis, information about HVV anomalous couplings both in VBF $+ VH$ production and in $H \to VV \to 4\ell$ decay is used. In all cases, the signal strength parameters are profiled, and the parameters common to the two analyses are correlated. The combined 68% C.L. and 95% C.L. intervals are presented in Table III, and the likelihood scans are shown in Fig. 11. While the constraints at large values of f_{ai} are predominantly driven by the decay information in the $H \to VV$ analysis, the constraints in the narrow range of f_{ai} near 0 are dominated by the production information where the $H \to \tau\tau$ channel

TABLE III. Allowed 68% C.L. (central values with uncertainties) and 95% C.L. (in square brackets) intervals on anomalous coupling parameters using a combination of the $H \to \tau\tau$ and $H \to 4\ell$ [17] decay channels.

Parameter	Observed/(10^{-3})		Expected/(10^{-3})	
	68% C.L.	95% C.L.	68% C.L.	95% C.L.
$f_{a3} \cos(\phi_{a3})$	0.00 ± 0.27	$[-92, 14]$	0.00 ± 0.23	$[-1.2, 1.2]$
$f_{a2} \cos(\phi_{a2})$	$0.08^{+1.04}_{-0.21}$	$[-1.1, 3.4]$	$0.0^{+1.3}_{-1.1}$	$[-4.0, 4.2]$
$f_{\Lambda 1} \cos(\phi_{\Lambda 1})$	$0.00^{+0.53}_{-0.09}$	$[-0.4, 1.8]$	$0.00^{+0.48}_{-0.12}$	$[-0.5, 1.7]$
$f_{\Lambda 1}^{Z\gamma} \cos(\phi_{\Lambda 1}^{Z\gamma})$	$0.0^{+1.1}_{-1.3}$	$[-6.5, 5.7]$	$0.0^{+2.6}_{-3.6}$	$[-11, 8.0]$

TABLE IV.   Summary of the allowed 95% C.L. intervals for the anomalous *HVV* couplings using the results in Table III. The coupling ratios are assumed to be real and include the factor $\cos(\phi_{\Lambda 1})$ or $\cos(\phi_{\Lambda 1}^{Z\gamma}) = \pm 1$.

Parameter	Observed	Expected
a_3/a_1	$[-0.81, 0.31]$	$[-0.090, 0.090]$
a_2/a_1	$[-0.055, 0.097]$	$[-0.11, 0.11]$
$(\Lambda_1 \sqrt{|a_1|}) \cos(\phi_{\Lambda 1})$ (GeV)	$[-\infty, -650] \cup [440, \infty]$	$[-\infty, -610] \cup [450, \infty]$
$(\Lambda_1^{Z\gamma} \sqrt{|a_1|}) \cos(\phi_{\Lambda 1}^{Z\gamma})$ (GeV)	$[-\infty, -400] \cup [420, \infty]$	$[-\infty, -360] \cup [390, \infty]$

dominates over the $H \to 4\ell$. This results in the most stringent limits on anomalous *HVV* couplings. Reverting the transformation in Eq. (3) [17], the $f_{ai} \cos(\phi_{ai})$ results can be interpreted for the coupling parameters used in Eq. (2), as shown in Table IV.

IX. CONCLUSIONS

A study is presented of anomalous *HVV* interactions of the *H* boson with vector bosons *V*, including *CP* violation, using its associated production with two hadronic jets in vector boson fusion, in the *VH* process, and in gluon fusion, and subsequently decaying to a pair of τ leptons. Constraints on the *CP*-violating parameter $f_{a3} \cos(\phi_{a3})$ and on the *CP*-conserving parameters $f_{a2} \cos(\phi_{a2})$, $f_{\Lambda 1} \cos(\phi_{\Lambda 1})$, and $f_{\Lambda 1}^{Z\gamma} \cos(\phi_{\Lambda 1}^{Z\gamma})$, defined in Eqs. (2) and (3), are set using matrix element techniques. The observed and expected limits on the parameters are summarized in Table II. The 68% confidence level constraints are generally tighter than those from previous measurements using either production or decay information. Further constraints are obtained in the combination of the $H \to \tau\tau$ and $H \to 4\ell$ decay [17] channels and are summarized in Table III. This combination places the most stringent constraints on anomalous *H* boson couplings: $f_{a3} \cos(\phi_{a3}) = (0.00 \pm 0.27) \times 10^{-3}$, $f_{a2} \cos(\phi_{a2}) = (0.08^{+1.04}_{-0.21}) \times 10^{-3}$, $f_{\Lambda 1} \cos(\phi_{\Lambda 1}) = (0.00^{+0.53}_{-0.09}) \times 10^{-3}$, and $f_{\Lambda 1}^{Z\gamma} \cos(\phi_{\Lambda 1}^{Z\gamma}) = (0.0^{+1.1}_{-1.3}) \times 10^{-3}$. A simultaneous measurement of $f_{a3} \cos(\phi_{a3})$ and $f_{a3}^{ggH} \cos(\phi_{a3}^{ggH})$ parameters is performed, where the latter parameter, defined in Eqs. (2) and (4), is sensitive to *CP*-violation effects in the gluon fusion process. The current dataset does not allow for precise constraints on *CP* properties in the gluon fusion process. The results are consistent with expectations for the standard model *H* boson.

[1] ATLAS Collaboration, Observation of a new particle in the search for the Standard Model Higgs boson with the ATLAS detector at the LHC, Phys. Lett. B **716**, 1 (2012).

[2] CMS Collaboration, Observation of a new boson at a mass of 125 GeV with the CMS experiment at the LHC, Phys. Lett. B **716**, 30 (2012).

[3] CMS Collaboration, Observation of a new boson with mass near 125 GeV in pp collisions at $\sqrt{s} = 7$ and 8 TeV, J. High Energy Phys. 06 (2013) 081.

[4] S. L. Glashow, Partial-symmetries of weak interactions, Nucl. Phys. **22**, 579 (1961).

[5] F. Englert and R. Brout, Broken Symmetry and the Mass of Gauge Vector Mesons, Phys. Rev. Lett. **13**, 321 (1964).

[6] P. W. Higgs, Broken symmetries, massless particles and gauge fields, Phys. Lett. **12**, 132 (1964).

[7] P. W. Higgs, Broken Symmetries and the Masses of Gauge Bosons, Phys. Rev. Lett. **13**, 508 (1964).

[8] G. S. Guralnik, C. R. Hagen, and T. W. B. Kibble, Global Conservation Laws and Massless Particles, Phys. Rev. Lett. **13**, 585 (1964).

[9] S. Weinberg, A Model of Leptons, Phys. Rev. Lett. **19**, 1264 (1967).

[10] A. Salam, Weak and electromagnetic interactions, in *Elementary Particle Physics: Relativistic Groups and Analyticity*, edited by N. Svartholm (Almqvist & Wiksell, Stockholm, 1968), p. 367, Proceedings of the Eighth Nobel Symposium.

[11] CMS Collaboration, On the Mass and Spin-Parity of the Higgs Boson Candidate Via its Decays to Z Boson Pairs, Phys. Rev. Lett. **110**, 081803 (2013).

[12] CMS Collaboration, Measurement of the properties of a Higgs boson in the four-lepton final state, Phys. Rev. D **89**, 092007 (2014).

[13] CMS Collaboration, Constraints on the spin-parity and anomalous HVV couplings of the Higgs boson in proton collisions at 7 and 8 TeV, Phys. Rev. D **92**, 012004 (2015).

[14] CMS Collaboration, Limits on the Higgs boson lifetime and width from its decay to four charged leptons, Phys. Rev. D **92**, 072010 (2015).

[15] CMS Collaboration, Combined search for anomalous pseudoscalar HVV couplings in $VH(H \to b\bar{b})$ production and $H \to VV$ decay, Phys. Lett. B **759**, 672 (2016).

[16] CMS Collaboration, Constraints on anomalous Higgs boson couplings using production and decay information in the four-lepton final state, Phys. Lett. B **775**, 1 (2017).

[17] CMS Collaboration, Measurements of the Higgs boson width and anomalous HVV couplings from on-shell and off-shell production in the four-lepton final state, Phys. Rev. D **99**, 112003 (2019).

[18] ATLAS Collaboration, Evidence for the spin-0 nature of the Higgs boson using ATLAS data, Phys. Lett. B **726**, 120 (2013).

[19] ATLAS Collaboration, Study of the spin and parity of the Higgs boson in diboson decays with the ATLAS detector, Eur. Phys. J. C **75**, 476 (2015).

[20] ATLAS Collaboration, Test of CP invariance in vector-boson fusion production of the Higgs boson using the optimal observable method in the ditau decay channel with the ATLAS detector, Eur. Phys. J. C **76**, 658 (2016).

[21] ATLAS Collaboration, Measurement of inclusive and differential cross sections in the $H \to ZZ^* \to 4\ell$ decay channel in pp collisions at $\sqrt{s} = 13$ TeV with the ATLAS detector, J. High Energy Phys. 10 (2017) 132.

[22] ATLAS Collaboration, Measurement of the Higgs boson coupling properties in the $H \to ZZ^* \to 4\ell$ decay channel at $\sqrt{s} = 13$ TeV with the ATLAS detector, J. High Energy Phys. 03 (2018) 095.

[23] ATLAS Collaboration, Measurements of Higgs boson properties in the diphoton decay channel with 36 fb^{-1} of pp collision data at $\sqrt{s} = 13$ TeV with the ATLAS detector, Phys. Rev. D **98**, 052005 (2018).

[24] CMS Collaboration, Observation of the Higgs boson decay to a pair of τ leptons with the CMS detector, Phys. Lett. B **779**, 283 (2018).

[25] S. Dawson *et al.*, Higgs working group report of the Snowmass 2013 community planning study, arXiv:1310.8361.

[26] Y. Gao, A. V. Gritsan, Z. Guo, K. Melnikov, M. Schulze, and N. V. Tran, Spin determination of single-produced

resonances at hadron colliders, Phys. Rev. D **81,** 075022 (2010).

[27] S. Bolognesi, Y. Gao, A. V. Gritsan, K. Melnikov, M. Schulze, N. V. Tran, and A. Whitbeck, Spin and parity of a single-produced resonance at the LHC, Phys. Rev. D **86,** 095031 (2012).

[28] I. Anderson, S. Bolognesi, F. Caola, Y. Gao, A. V. Gritsan, C. B. Martin, K. Melnikov, M. Schulze, N. V. Tran, A. Whitbeck, and Y. Zhou, Constraining anomalous HVV interactions at proton and lepton colliders, Phys. Rev. D **89,** 035007 (2014).

[29] A. V. Gritsan, R. Röntsch, M. Schulze, and M. Xiao, Constraining anomalous Higgs boson couplings to the heavy flavor fermions using matrix element techniques, Phys. Rev. D **94,** 055023 (2016).

[30] CMS Collaboration, The CMS trigger system, J. Instrum. **12,** P01020 (2017).

[31] CMS Collaboration, The CMS experiment at the CERN LHC, J. Instrum. **3,** S08004 (2008).

[32] CMS Collaboration, Particle-flow reconstruction and global event description with the CMS detector, J. Instrum. **12,** P10003 (2017).

[33] M. Cacciari, G. P. Salam, and G. Soyez, The anti-k_T jet clustering algorithm, J. High Energy Phys. 04 (2008) 063.

[34] M. Cacciari, G. P. Salam, and G. Soyez, FastJet user manual, Eur. Phys. J. C **72,** 1896 (2012).

[35] CMS Collaboration, Performance of electron reconstruction and selection with the CMS detector in proton-proton collisions at $\sqrt{s} = 8$ TeV, J. Instrum. **10,** P06005 (2015).

[36] CMS Collaboration, Performance of the CMS muon detector and muon reconstruction with proton-proton collisons at $\sqrt{s} = 13$ TeV, J. Instrum. **13,** P06015 (2018).

[37] M. Cacciari and G. P. Salam, Dispelling the N^3 myth for the k_t jet-finder, Phys. Lett. B **641,** 57 (2006).

[38] CMS Collaboration, Reconstruction and identification of τ lepton decays to hadrons and ν_τ at CMS, J. Instrum. **11,** P01019 (2016).

[39] CMS Collaboration, Performance of reconstruction and identification of τ leptons decaying to hadrons and ν_τ in pp collisions at $\sqrt{s} = 13$ TeV, J. Instrum. **13,** P10005 (2018).

[40] CMS Collaboration, Performance of missing transverse momentum in pp collisions at $\sqrt{s} = 13$ TeV using the CMS detector, CMS physics analysis summary, CERN Report No. CMS-PAS-JME-17-001, 2018, http://cds.cern.ch/record/2628600.

[41] L. Bianchini, J. Conway, E. Klose Friis, and C. Veelken, Reconstruction of the Higgs mass in $H \rightarrow \tau\tau$ events by dynamical likelihood techniques, J. Phys. Conf. Ser. **513,** 022035 (2014).

[42] CMS Collaboration, Search for neutral MSSM Higgs bosons decaying to a pair of tau leptons in pp collisions, J. High Energy Phys. 10 (2014) 160.

[43] T. Plehn, D. L. Rainwater, and D. Zeppenfeld, Determining the Structure of Higgs Couplings at the LHC, Phys. Rev. Lett. **88,** 051801 (2002).

[44] V. Hankele, G. Klamke, D. Zeppenfeld, and T. Figy, Anomalous Higgs boson couplings in vector boson fusion at the CERN LHC, Phys. Rev. D **74,** 095001 (2006).

[45] E. Accomando *et al.*, *Workshop on CP Studies and Non-Standard Higgs Physics* (CERN, Geneva, Switzerland, 2006).

[46] K. Hagiwara, Q. Li, and K. Mawatari, Jet angular correlation in vector-boson fusion processes at hadron colliders, J. High Energy Phys. 07 (2009) 101.

[47] A. De Rújula, J. Lykken, M. Pierini, C. Rogan, and M. Spiropulu, Higgs look-alikes at the LHC, Phys. Rev. D **82,** 013003 (2010).

[48] J. Ellis, D. S. Hwang, V. Sanz, and T. You, A fast track towards the 'Higgs' spin and parity, J. High Energy Phys. 11 (2012) 134.

[49] P. Artoisenet, P. de Aquino, F. Demartin, R. Frederix, S. Frixione, F. Maltoni, M. K. Mandal, P. Mathews, K. Mawatari, V. Ravindran, S. Seth, P. Torrielli, and M. Zaro, A framework for Higgs characterisation, J. High Energy Phys. 11 (2013) 043.

[50] M. J. Dolan, P. Harris, M. Jankowiak, and M. Spannowsky, Constraining *CP*-violating Higgs sectors at the LHC using gluon fusion, Phys. Rev. D **90,** 073008 (2014).

[51] A. Greljo, G. Isidori, J. M. Lindert, and D. Marzocca, Pseudo-observables in electroweak Higgs production, Eur. Phys. J. C **76,** 158 (2016).

[52] S. Frixione, P. Nason, and C. Oleari, Matching NLO QCD computations with parton shower simulations: The POWHEG method, J. High Energy Phys. 11 (2007) 070.

[53] E. Bagnaschi, G. Degrassi, P. Slavich, and A. Vicini, Higgs production via gluon fusion in the POWHEG approach in the SM and in the MSSM, J. High Energy Phys. 02 (2012) 088.

[54] P. Nason and C. Oleari, NLO Higgs boson production via vector-boson fusion matched with shower in POWHEG, J. High Energy Phys. 02 (2010) 037.

[55] G. Luisoni, P. Nason, C. Oleari, and F. Tramontano, $HW^{\pm}/HZ + 0$ and 1 jet at NLO with the POWHEG BOX interfaced to GoSam and their merging within MiNLO, J. High Energy Phys. 10 (2013) 083.

[56] T. Sjostrand, S. Ask, J. R. Christiansen, R. Corke, N. Desai, P. Ilten, S. Mrenna, S. Prestel, C. O. Rasmussen, and P. Z. Skands, An introduction to PYTHIA 8.2, Comput. Phys. Commun. **191,** 159 (2015).

[57] R. D. Ball, V. Bertone, F. Cerutti, L. Del Debbio, S. Forte, A. Guffanti, J. I. Latorre, J. Rojo, and M. Ubiali (NNPDF), Unbiased global determination of parton distributions and their uncertainties at NNLO and at LO, Nucl. Phys. **B855,** 153 (2012).

[58] S. Agostinelli *et al.* (GEANT4 Collaboration), GEANT4—A simulation toolkit, Nucl. Instrum. Methods Phys. Res., Sect. A **506,** 250 (2003).

[59] J. Alwall, R. Frederix, S. Frixione, V. Hirschi, F. Maltoni, O. Mattelaer, H. S. Shao, T. Stelzer, P. Torrielli, and M. Zaro, The automated computation of tree-level and next-to-leading order differential cross sections, and their matching to parton shower simulations, J. High Energy Phys. 07 (2014) 079.

[60] J. Alwall, S. Höche, F. Krauss, N. Lavesson, L. Lönnblad, F. Maltoni, M. L. Mangano, M. Moretti, C. G. Papadopoulos, F. Piccinini, S. Schumann, M. Treccani, J. Winter, and M. Worek, Comparative study of various algorithms for the merging of parton showers and matrix elements in hadronic collisions, Eur. Phys. J. C **53,** 473 (2008).

[61] R. Frederix and S. Frixione, Merging meets matching in MC@NLO, J. High Energy Phys. 12 (2012) 061.

[62] CMS Collaboration, Event generator tunes obtained from underlying event and multiparton scattering measurements, Eur. Phys. J. C **76**, 155 (2016).

[63] J. Neyman and E. S. Pearson, On the problem of the most efficient tests of statistical hypotheses, Phil. Trans. R. Soc. A **231**, 289 (1933).

[64] R. J. Barlow, Extended maximum likelihood, Nucl. Instrum. Methods Phys. Res., Sect. A **297**, 496 (1990).

[65] W. Verkerke and D. P. Kirkby, The RooFit toolkit for data modeling, eConfC0303241, MOLT007 (2003).

[66] R. Brun and F. Rademakers, ROOT: An object oriented data analysis framework, Nucl. Instrum. Methods Phys. Res., Sect. A **389**, 81 (1997).

[67] S. S. Wilks, The large-sample distribution of the likelihood ratio for testing composite hypotheses, Ann. Math. Stat. **9**, 60 (1938).

[68] J. S. Conway, Incorporating nuisance parameters in likelihoods for multisource spectra, in *Proceedings of PHYS-TAT 2011 Workshop on Statistical Issues Related to Discovery Claims in Search Experiments and Unfolding* (CERN, Geneva, 2011), p. 115, CERN-2011-006.

[69] CMS Collaboration, Identification of heavy-flavour jets with the CMS detector in pp collisions at 13 TeV, J. Instrum. **13**, P05011 (2018).

[70] CMS Collaboration, Performance of the CMS missing transverse momentum reconstruction in pp data at $\sqrt{s} = 8$ TeV, J. Instrum. **10**, P02006 (2015).

[71] CMS Collaboration, CMS luminosity measurements for the 2016 data taking period, CMS physics analysis summary, CERN Report No. CMS-PAS-LUM-17-001, 2017, https://cds.cern.ch/record/2257069.

[72] D. de Florian *et al.*, Handbook of LHC Higgs cross sections: 4. Deciphering the nature of the Higgs sector, Technical Report No. CERN-2017-002-M (2016), https://doi.org/10.23731/CYRM-2017-002.

[73] CMS Collaboration, Measurements of the $pp \to ZZ$ production cross section and the $Z \to 4\ell$ branching fraction, and constraints on anomalous triple gauge couplings at $\sqrt{s} = 13$ TeV, Eur. Phys. J. C **78**, 165 (2018).

[74] CMS Collaboration, Cross section measurement of t-channel single top quark production in pp collisions at $\sqrt{s} = 13$ TeV, Phys. Lett. B **772**, 752 (2017).

A. M. Sirunyan,[1] A. Tumasyan,[1] W. Adam,[2] F. Ambrogi,[2] E. Asilar,[2] T. Bergauer,[2] J. Brandstetter,[2] M. Dragicevic,[2] J. Erö,[2] A. Escalante Del Valle,[2] M. Flechl,[2] R. Frühwirth,[2,b] V. M. Ghete,[2] J. Hrubec,[2] M. Jeitler,[2,b] N. Krammer,[2] I. Krätschmer,[2] D. Liko,[2] T. Madlener,[2] I. Mikulec,[2] N. Rad,[2] H. Rohringer,[2] J. Schieck,[2,b] R. Schöfbeck,[2] M. Spanring,[2] D. Spitzbart,[2] W. Waltenberger,[2] J. Wittmann,[2] C.-E. Wulz,[2,b] M. Zarucki,[2] V. Chekhovsky,[3] V. Mossolov,[3] J. Suarez Gonzalez,[3] E. A. De Wolf,[4] D. Di Croce,[4] X. Janssen,[4] J. Lauwers,[4] A. Lelek,[4] M. Pieters,[4] H. Van Haevermaet,[4] P. Van Mechelen,[4] N. Van Remortel,[4] F. Blekman,[5] J. D'Hondt,[5] J. De Clercq,[5] K. Deroover,[5] G. Flouris,[5] D. Lontkovskyi,[5] S. Lowette,[5] I. Marchesini,[5] S. Moortgat,[5] L. Moreels,[5] Q. Python,[5] K. Skovpen,[5] S. Tavernier,[5] W. Van Doninck,[5] P. Van Mulders,[5] I. Van Parijs,[5] D. Beghin,[6] B. Bilin,[6] H. Brun,[6] B. Clerbaux,[6] G. De Lentdecker,[6] H. Delannoy,[6] B. Dorney,[6] G. Fasanella,[6] L. Favart,[6] A. Grebenyuk,[6] A. K. Kalsi,[6] J. Luetic,[6] N. Postiau,[6] E. Starling,[6] L. Thomas,[6] C. Vander Velde,[6] P. Vanlaer,[6] D. Vannerom,[6] Q. Wang,[6] T. Cornelis,[7] D. Dobur,[7] A. Fagot,[7] M. Gul,[7] I. Khvastunov,[7,c] C. Roskas,[7] D. Trocino,[7] M. Tytgat,[7] W. Verbeke,[7] B. Vermassen,[7] M. Vit,[7] N. Zaganidis,[7] H. Bakhshiansohi,[8] O. Bondu,[8] G. Bruno,[8] C. Caputo,[8] P. David,[8] C. Delaere,[8] M. Delcourt,[8] A. Giammanco,[8] G. Krintiras,[8] V. Lemaitre,[8] A. Magitteri,[8] K. Piotrzkowski,[8] A. Saggio,[8] M. Vidal Marono,[8] P. Vischia,[8] J. Zobec,[8] F. L. Alves,[9] G. A. Alves,[9] G. Correia Silva,[9] C. Hensel,[9] A. Moraes,[9] M. E. Pol,[9] P. Rebello Teles,[9] E. Belchior Batista Das Chagas,[10] W. Carvalho,[10] J. Chinellato,[10,d] E. Coelho,[10] E. M. Da Costa,[10] G. G. Da Silveira,[10,e] D. De Jesus Damiao,[10] C. De Oliveira Martins,[10] S. Fonseca De Souza,[10] L. M. Huertas Guativa,[10] H. Malbouisson,[10] D. Matos Figueiredo,[10] M. Melo De Almeida,[10] C. Mora Herrera,[10] L. Mundim,[10] H. Nogima,[10] W. L. Prado Da Silva,[10] L. J. Sanchez Rosas,[10] A. Santoro,[10] A. Sznajder,[10] M. Thiel,[10] E. J. Tonelli Manganote,[10,d] F. Torres Da Silva De Araujo,[10] A. Vilela Pereira,[10] S. Ahuja,[11a] C. A. Bernardes,[11a] L. Calligaris,[11a] T. R. Fernandez Perez Tomei,[11a] E. M. Gregores,[11a,11b] P. G. Mercadante,[11a,11b] S. F. Novaes,[11a] Sandra S. Padula,[11a] A. Aleksandrov,[12] R. Hadjiiska,[12] P. Iaydjiev,[12] A. Marinov,[12] M. Misheva,[12] M. Rodozov,[12] M. Shopova,[12] G. Sultanov,[12] A. Dimitrov,[13] L. Litov,[13] B. Pavlov,[13] P. Petkov,[13] W. Fang,[14,f] X. Gao,[14,f] L. Yuan,[14] M. Ahmad,[15] J. G. Bian,[15] G. M. Chen,[15] H. S. Chen,[15] M. Chen,[15] Y. Chen,[15] C. H. Jiang,[15] D. Leggat,[15] H. Liao,[15] Z. Liu,[15] S. M. Shaheen,[15,g] A. Spiezia,[15] J. Tao,[15] E. Yazgan,[15] H. Zhang,[15] S. Zhang,[15,g] J. Zhao,[15] Y. Ban,[16] G. Chen,[16] A. Levin,[16] J. Li,[16] L. Li,[16] Q. Li,[16] Y. Mao,[16] S. J. Qian,[16] D. Wang,[16] Y. Wang,[17] C. Avila,[18] A. Cabrera,[18] C. A. Carrillo Montoya,[18] L. F. Chaparro Sierra,[18] C. Florez,[18] C. F. González Hernández,[18] M. A. Segura Delgado,[18] N. Godinovic,[19] D. Lelas,[19] I. Puljak,[19] T. Sculac,[19] Z. Antunovic,[20] M. Kovac,[20] V. Brigljevic,[21] D. Ferencek,[21] K. Kadija,[21] B. Mesic,[21] M. Roguljic,[21] A. Starodumov,[21,h] T. Susa,[21] M. W. Ather,[22] A. Attikis,[22] M. Kolosova,[22] G. Mavromanolakis,[22] J. Mousa,[22] C. Nicolaou,[22] F. Ptochos,[22] P. A. Razis,[22] H. Rykaczewski,[22] M. Finger,[23,i] M. Finger Jr.,[23,i] E. Ayala,[24] E. Carrera Jarrin,[25] A. A. Abdelalim,[26,j,k] Y. Assran,[26,l,m] M. A. Mahmoud,[26,l,n] S. Bhowmik,[27] A. Carvalho Antunes De Oliveira,[27]

R. K. Dewanjee,[27] K. Ehataht,[27] M. Kadastik,[27] M. Raidal,[27] C. Veelken,[27] P. Eerola,[28] H. Kirschenmann,[28] J. Pekkanen,[28] M. Voutilainen,[28] J. Havukainen,[29] J. K. Heikkilä,[29] T. Järvinen,[29] V. Karimäki,[29] R. Kinnunen,[29] T. Lampén,[29] K. Lassila-Perini,[29] S. Laurila,[29] S. Lehti,[29] T. Lindén,[29] P. Luukka,[29] T. Mäenpää,[29] H. Siikonen,[29] E. Tuominen,[29] J. Tuominiemi,[29] T. Tuuva,[30] M. Besancon,[31] F. Couderc,[31] M. Dejardin,[31] D. Denegri,[31] J. L. Faure,[31] F. Ferri,[31] S. Ganjour,[31] A. Givernaud,[31] P. Gras,[31] G. Hamel de Monchenault,[31] P. Jarry,[31] C. Leloup,[31] E. Locci,[31] J. Malcles,[31] G. Negro,[31] J. Rander,[31] A. Rosowsky,[31] M. Ö. Sahin,[31] M. Titov,[31] A. Abdulsalam,[32,o] C. Amendola,[32] I. Antropov,[32] F. Beaudette,[32] P. Busson,[32] C. Charlot,[32] B. Diab,[32] R. Granier de Cassagnac,[32] I. Kucher,[32] A. Lobanov,[32] J. Martin Blanco,[32] C. Martin Perez,[32] M. Nguyen,[32] C. Ochando,[32] G. Ortona,[32] P. Paganini,[32] J. Rembser,[32] R. Salerno,[32] J. B. Sauvan,[32] Y. Sirois,[32] A. G. Stahl Leiton,[32] A. Zabi,[32] A. Zghiche,[32] J.-L. Agram,[33,p] J. Andrea,[33] D. Bloch,[33] G. Bourgatte,[33] J.-M. Brom,[33] E. C. Chabert,[33] V. Cherepanov,[33] C. Collard,[33] E. Conte,[33,p] J.-C. Fontaine,[33,p] D. Gelé,[33] U. Goerlach,[33] M. Jansová,[33] A.-C. Le Bihan,[33] N. Tonon,[33] P. Van Hove,[33] S. Gadrat,[34] S. Beauceron,[35] C. Bernet,[35] G. Boudoul,[35] N. Chanon,[35] R. Chierici,[35] D. Contardo,[35] P. Depasse,[35] H. El Mamouni,[35] J. Fay,[35] S. Gascon,[35] M. Gouzevitch,[35] G. Grenier,[35] B. Ille,[35] F. Lagarde,[35] I. B. Laktineh,[35] H. Lattaud,[35] M. Lethuillier,[35] L. Mirabito,[35] S. Perries,[35] A. Popov,[35,q] V. Sordini,[35] G. Touquet,[35] M. Vander Donckt,[35] S. Viret,[35] A. Khvedelidze,[36,i] Z. Tsamalaidze,[37,i] C. Autermann,[38] L. Feld,[38] M. K. Kiesel,[38] K. Klein,[38] M. Lipinski,[38] M. Preuten,[38] M. P. Rauch,[38] C. Schomakers,[38] J. Schulz,[38] M. Teroerde,[38] B. Wittmer,[38] A. Albert,[39] M. Erdmann,[39] S. Erdweg,[39] T. Esch,[39] R. Fischer,[39] S. Ghosh,[39] T. Hebbeker,[39] C. Heidemann,[39] K. Hoepfner,[39] H. Keller,[39] L. Mastrolorenzo,[39] M. Merschmeyer,[39] A. Meyer,[39] P. Millet,[39] S. Mukherjee,[39] A. Novak,[39] T. Pook,[39] A. Pozdnyakov,[39] M. Radziej,[39] H. Reithler,[39] M. Rieger,[39] A. Schmidt,[39] D. Teyssier,[39] S. Thüer,[39] G. Flügge,[40] O. Hlushchenko,[40] T. Kress,[40] T. Müller,[40] A. Nehrkorn,[40] A. Nowack,[40] C. Pistone,[40] O. Pooth,[40] D. Roy,[40] H. Sert,[40] A. Stahl,[40,r] M. Aldaya Martin,[41] T. Arndt,[41] C. Asawatangtrakuldee,[41] I. Babounikau,[41] K. Beernaert,[41] O. Behnke,[41] U. Behrens,[41] A. Bermúdez Martínez,[41] D. Bertsche,[41] A. A. Bin Anuar,[41] K. Borras,[41,s] V. Botta,[41] A. Campbell,[41] P. Connor,[41] C. Contreras-Campana,[41] V. Danilov,[41] A. De Wit,[41] M. M. Defranchis,[41] C. Diez Pardos,[41] D. Domínguez Damiani,[41] G. Eckerlin,[41] T. Eichhorn,[41] A. Elwood,[41] E. Eren,[41] E. Gallo,[41,t] A. Geiser,[41] J. M. Grados Luyando,[41] A. Grohsjean,[41] M. Guthoff,[41] M. Haranko,[41] A. Harb,[41] H. Jung,[41] M. Kasemann,[41] J. Keaveney,[41] C. Kleinwort,[41] J. Knolle,[41] D. Krücker,[41] W. Lange,[41] T. Lenz,[41] J. Leonard,[41] K. Lipka,[41] W. Lohmann,[41,u] R. Mankel,[41] I.-A. Melzer-Pellmann,[41] A. B. Meyer,[41] M. Meyer,[41] M. Missiroli,[41] G. Mittag,[41] J. Mnich,[41] V. Myronenko,[41] S. K. Pflitsch,[41] D. Pitzl,[41] A. Raspereza,[41] A. Saibel,[41] M. Savitskyi,[41] P. Saxena,[41] P. Schütze,[41] C. Schwanenberger,[41] R. Shevchenko,[41] A. Singh,[41] H. Tholen,[41] O. Turkot,[41] A. Vagnerini,[41] M. Van De Klundert,[41] G. P. Van Onsem,[41] R. Walsh,[41] Y. Wen,[41] K. Wichmann,[41] C. Wissing,[41] O. Zenaiev,[41] R. Aggleton,[42] S. Bein,[42] L. Benato,[42] A. Benecke,[42] V. Blobel,[42] T. Dreyer,[42] A. Ebrahimi,[42] E. Garutti,[42] D. Gonzalez,[42] P. Gunnellini,[42] J. Haller,[42] A. Hinzmann,[42] A. Karavdina,[42] G. Kasieczka,[42] R. Klanner,[42] R. Kogler,[42] N. Kovalchuk,[42] S. Kurz,[42] V. Kutzner,[42] J. Lange,[42] D. Marconi,[42] J. Multhaup,[42] M. Niedziela,[42] C. E. N. Niemeyer,[42] D. Nowatschin,[42] A. Perieanu,[42] A. Reimers,[42] O. Rieger,[42] C. Scharf,[42] P. Schleper,[42] S. Schumann,[42] J. Schwandt,[42] J. Sonneveld,[42] H. Stadie,[42] G. Steinbrück,[42] F. M. Stober,[42] M. Stöver,[42] B. Vormwald,[42] I. Zoi,[42] M. Akbiyik,[43] C. Barth,[43] M. Baselga,[43] S. Baur,[43] E. Butz,[43] R. Caspart,[43] T. Chwalek,[43] F. Colombo,[43] W. De Boer,[43] A. Dierlamm,[43] K. El Morabit,[43] N. Faltermann,[43] B. Freund,[43] M. Giffels,[43] M. A. Harrendorf,[43] F. Hartmann,[43,r] S. M. Heindl,[43] U. Husemann,[43] I. Katkov,[43,q] S. Kudella,[43] S. Mitra,[43] M. U. Mozer,[43] Th. Müller,[43] M. Musich,[43] M. Plagge,[43] G. Quast,[43] K. Rabbertz,[43] M. Schröder,[43] I. Shvetsov,[43] H. J. Simonis,[43] R. Ulrich,[43] S. Wayand,[43] M. Weber,[43] T. Weiler,[43] C. Wöhrmann,[43] R. Wolf,[43] G. Anagnostou,[44] G. Daskalakis,[44] T. Geralis,[44] A. Kyriakis,[44] D. Loukas,[44] G. Paspalaki,[44] A. Agapitos,[45] G. Karathanasis,[45] P. Kontaxakis,[45] A. Panagiotou,[45] I. Papavergou,[45] N. Saoulidou,[45] K. Vellidis,[45] G. Bakas,[46] K. Kousouris,[46] I. Papakrivopoulos,[46] G. Tsipolitis,[46] I. Evangelou,[47] C. Foudas,[47] P. Gianneios,[47] P. Katsoulis,[47] P. Kokkas,[47] S. Mallios,[47] K. Manitara,[47] N. Manthos,[47] I. Papadopoulos,[47] E. Paradas,[47] J. Strologas,[47] F. A. Triantis,[47] D. Tsitsonis,[47] M. Bartók,[48,v] M. Csanad,[48] N. Filipovic,[48] P. Major,[48] K. Mandal,[48] A. Mehta,[48] M. I. Nagy,[48] G. Pasztor,[48] O. Surányi,[48] G. I. Veres,[48] G. Bencze,[49] C. Hajdu,[49] D. Horvath,[49,w] Á. Hunyadi,[49] F. Sikler,[49] T. Á. Vámi,[49] V. Veszpremi,[49] G. Vesztergombi,[49,a,x] N. Beni,[50] S. Czellar,[50] J. Karancsi,[50,v] A. Makovec,[50] J. Molnar,[50] Z. Szillasi,[50] P. Raics,[51] Z. L. Trocsanyi,[51] B. Ujvari,[51] S. Choudhury,[52] J. R. Komaragiri,[52] P. C. Tiwari,[52] S. Bahinipati,[53,y] C. Kar,[53] P. Mal,[53] A. Nayak,[53,z] S. Roy Chowdhury,[53] D. K. Sahoo,[53,y] S. K. Swain,[53] S. Bansal,[54] S. B. Beri,[54] V. Bhatnagar,[54] S. Chauhan,[54] R. Chawla,[54] N. Dhingra,[54] R. Gupta,[54] A. Kaur,[54] M. Kaur,[54] S. Kaur,[54] P. Kumari,[54] M. Lohan,[54] M. Meena,[54] K. Sandeep,[54] S. Sharma,[54] J. B. Singh,[54] A. K. Virdi,[54] G. Walia,[54] A. Bhardwaj,[55] B. C. Choudhary,[55] R. B. Garg,[55] M. Gola,[55] S. Keshri,[55]

Ashok Kumar,[55] S. Malhotra,[55] M. Naimuddin,[55] P. Priyanka,[55] K. Ranjan,[55] Aashaq Shah,[55] R. Sharma,[55] R. Bhardwaj,[56,aa] M. Bharti,[56,aa] R. Bhattacharya,[56] S. Bhattacharya,[56] U. Bhawandeep,[56,aa] D. Bhowmik,[56] S. Dey,[56] S. Dutt,[56,aa] S. Dutta,[56] S. Ghosh,[56] M. Maity,[56,bb] K. Mondal,[56] S. Nandan,[56] A. Purohit,[56] P. K. Rout,[56] A. Roy,[56] G. Saha,[56] S. Sarkar,[56] T. Sarkar,[56,bb] M. Sharan,[56] B. Singh,[56,aa] S. Thakur,[56,aa] P. K. Behera,[57] A. Muhammad,[57] R. Chudasama,[58] D. Dutta,[58] V. Jha,[58] V. Kumar,[58] D. K. Mishra,[58] P. K. Netrakanti,[58] L. M. Pant,[58] P. Shukla,[58] P. Suggisetti,[58] T. Aziz,[59] M. A. Bhat,[59] S. Dugad,[59] G. B. Mohanty,[59] N. Sur,[59] Ravindra Kumar Verma,[59] S. Banerjee,[60] S. Bhattacharya,[60] S. Chatterjee,[60] P. Das,[60] M. Guchait,[60] Sa. Jain,[60] S. Karmakar,[60] S. Kumar,[60] G. Majumder,[60] K. Mazumdar,[60] N. Sahoo,[60] S. Chauhan,[61] S. Dube,[61] V. Hegde,[61] A. Kapoor,[61] K. Kothekar,[61] S. Pandey,[61] A. Rane,[61] A. Rastogi,[61] S. Sharma,[61] S. Chenarani,[62,cc] E. Eskandari Tadavani,[62] S. M. Etesami,[62,cc] M. Khakzad,[62] M. Mohammadi Najafabadi,[62] M. Naseri,[62] F. Rezaei Hosseinabadi,[62] B. Safarzadeh,[62,dd] M. Zeinali,[62] M. Felcini,[63] M. Grunewald,[63] M. Abbrescia,[64a,64b] C. Calabria,[64a,64b] A. Colaleo,[64a] D. Creanza,[64a,64c] L. Cristella,[64a,64b] N. De Filippis,[64a,64c] M. De Palma,[64a,64b] A. Di Florio,[64a,64b] F. Errico,[64a,64b] L. Fiore,[64a] A. Gelmi,[64a,64b] G. Iaselli,[64a,64c] M. Ince,[64a,64b] S. Lezki,[64a,64b] G. Maggi,[64a,64c] M. Maggi,[64a] G. Miniello,[64a,64b] S. My,[64a,64b] S. Nuzzo,[64a,64b] A. Pompili,[64a,64b] G. Pugliese,[64a,64c] R. Radogna,[64a] A. Ranieri,[64a] G. Selvaggi,[64a,64b] A. Sharma,[64a] L. Silvestris,[64a] R. Venditti,[64a] P. Verwilligen,[64a] G. Abbiendi,[65a] C. Battilana,[65a,65b] D. Bonacorsi,[65a,65b] L. Borgonovi,[65a,65b] S. Braibant-Giacomelli,[65a,65b] R. Campanini,[65a,65b] P. Capiluppi,[65a,65b] A. Castro,[65a,65b] F. R. Cavallo,[65a] S. S. Chhibra,[65a,65b] G. Codispoti,[65a,65b] M. Cuffiani,[65a,65b] G. M. Dallavalle,[65a] F. Fabbri,[65a] A. Fanfani,[65a,65b] E. Fontanesi,[65a] P. Giacomelli,[65a] C. Grandi,[65a] L. Guiducci,[65a,65b] F. Iemmi,[65a,65b] S. Lo Meo,[65a,ee] S. Marcellini,[65a] G. Masetti,[65a] A. Montanari,[65a] F. L. Navarria,[65a,65b] A. Perrotta,[65a] F. Primavera,[65a,65b] A. M. Rossi,[65a,65b] T. Rovelli,[65a,65b] G. P. Siroli,[65a,65b] N. Tosi,[65a] S. Albergo,[66a,66b,ff] A. Di Mattia,[66a] R. Potenza,[66a,66b] A. Tricomi,[66a,66b,ff] C. Tuve,[66a,66b] G. Barbagli,[67a] K. Chatterjee,[67a,67b] V. Ciulli,[67a,67b] C. Civinini,[67a] R. D'Alessandro,[67a,67b] E. Focardi,[67a,67b] G. Latino,[67a] P. Lenzi,[67a,67b] M. Meschini,[67a] S. Paoletti,[67a] L. Russo,[67a,gg] G. Sguazzoni,[67a] D. Strom,[67a] L. Viliani,[67a] L. Benussi,[68] S. Bianco,[68] F. Fabbri,[68] D. Piccolo,[68] F. Ferro,[69a] R. Mulargia,[69a,69b] E. Robutti,[69a] S. Tosi,[69a,69b] A. Benaglia,[70a] A. Beschi,[70a,70b] F. Brivio,[70a,70b] V. Ciriolo,[70a,70b,r] S. Di Guida,[70a,70b,r] M. E. Dinardo,[70a,70b] S. Fiorendi,[70a,70b] S. Gennai,[70a] A. Ghezzi,[70a,70b] P. Govoni,[70a,70b] M. Malberti,[70a,70b] S. Malvezzi,[70a] D. Menasce,[70a] F. Monti,[70a] L. Moroni,[70a] M. Paganoni,[70a,70b] D. Pedrini,[70a] S. Ragazzi,[70a,70b] T. Tabarelli de Fatis,[70a,70b] D. Zuolo,[70a,70b] S. Buontempo,[71a] N. Cavallo,[71a,71c] A. De Iorio,[71a,71b] A. Di Crescenzo,[71a,71b] F. Fabozzi,[71a,71c] F. Fienga,[71a] G. Galati,[71a] A. O. M. Iorio,[71a,71b] L. Lista,[71a] S. Meola,[71a,71d,r] P. Paolucci,[71a,r] C. Sciacca,[71a,71b] E. Voevodina,[71a,71b] P. Azzi,[72a] N. Bacchetta,[72a] D. Bisello,[72a,72b] A. Boletti,[72a,72b] A. Bragagnolo,[72a] R. Carlin,[72a,72b] P. Checchia,[72a] M. Dall'Osso,[72a,72b] P. De Castro Manzano,[72a] T. Dorigo,[72a] U. Dosselli,[72a] F. Gasparini,[72a,72b] U. Gasparini,[72a,72b] A. Gozzelino,[72a] S. Y. Hoh,[72a] S. Lacaprara,[72a] P. Lujan,[72a] M. Margoni,[72a,72b] A. T. Meneguzzo,[72a,72b] J. Pazzini,[72a,72b] M. Presilla,[72a,72b] P. Ronchese,[72a,72b] R. Rossin,[72a,72b] F. Simonetto,[72a,72b] A. Tiko,[72a] E. Torassa,[72a] M. Tosi,[72a,72b] M. Zanetti,[72a,72b] P. Zotto,[72a,72b] G. Zumerle,[72a,72b] A. Braghieri,[73a] A. Magnani,[73a] P. Montagna,[73a,73b] S. P. Ratti,[73a,73b] V. Re,[73a] M. Ressegotti,[73a,73b] C. Riccardi,[73a,73b] P. Salvini,[73a] I. Vai,[73a,73b] P. Vitulo,[73a,73b] M. Biasini,[74a,74b] G. M. Bilei,[74a] C. Cecchi,[74a,74b] D. Ciangottini,[74a,74b] L. Fanò,[74a,74b] P. Lariccia,[74a,74b] R. Leonardi,[74a,74b] E. Manoni,[74a] G. Mantovani,[74a,74b] V. Mariani,[74a,74b] M. Menichelli,[74a] A. Rossi,[74a,74b] A. Santocchia,[74a,74b] D. Spiga,[74a] K. Androsov,[75a] P. Azzurri,[75a] G. Bagliesi,[75a] L. Bianchini,[75a] T. Boccali,[75a] L. Borrello,[75a] R. Castaldi,[75a] M. A. Ciocci,[75a,75b] R. Dell'Orso,[75a] G. Fedi,[75a] F. Fiori,[75a,75c] L. Giannini,[75a,75c] A. Giassi,[75a] M. T. Grippo,[75a] F. Ligabue,[75a,75c] E. Manca,[75a,75c] G. Mandorli,[75a,75c] A. Messineo,[75a,75b] F. Palla,[75a] A. Rizzi,[75a,75b] G. Rolandi,[75a,hh] P. Spagnolo,[75a] R. Tenchini,[75a] G. Tonelli,[75a,75b] A. Venturi,[75a] P. G. Verdini,[75a] L. Barone,[76a,76b] F. Cavallari,[76a] M. Cipriani,[76a,76b] D. Del Re,[76a,76b] E. Di Marco,[76a,76b] M. Diemoz,[76a] S. Gelli,[76a,76b] E. Longo,[76a,76b] B. Marzocchi,[76a,76b] P. Meridiani,[76a] G. Organtini,[76a,76b] F. Pandolfi,[76a] R. Paramatti,[76a,76b] F. Preiato,[76a,76b] S. Rahatlou,[76a,76b] C. Rovelli,[76a] F. Santanastasio,[76a,76b] N. Amapane,[77a,77b] R. Arcidiacono,[77a,77c] S. Argiro,[77a,77b] M. Arneodo,[77a,77c] N. Bartosik,[77a] R. Bellan,[77a,77b] C. Biino,[77a] A. Cappati,[77a,77b] N. Cartiglia,[77a] F. Cenna,[77a,77b] S. Cometti,[77a] M. Costa,[77a,77b] R. Covarelli,[77a,77b] N. Demaria,[77a] B. Kiani,[77a,77b] C. Mariotti,[77a] S. Maselli,[77a] E. Migliore,[77a,77b] V. Monaco,[77a,77b] E. Monteil,[77a,77b] M. Monteno,[77a] M. M. Obertino,[77a,77b] L. Pacher,[77a,77b] N. Pastrone,[77a] M. Pelliccioni,[77a] G. L. Pinna Angioni,[77a,77b] A. Romero,[77a,77b] M. Ruspa,[77a,77c] R. Sacchi,[77a,77b] R. Salvatico,[77a,77b] K. Shchelina,[77a,77b] V. Sola,[77a] A. Solano,[77a,77b] D. Soldi,[77a,77b] A. Staiano,[77a] S. Belforte,[78a] V. Candelise,[78a,78b] M. Casarsa,[78a] F. Cossutti,[78a] A. Da Rold,[78a,78b] G. Della Ricca,[78a,78b] F. Vazzoler,[78a,78b] A. Zanetti,[78a] D. H. Kim,[79] G. N. Kim,[79] M. S. Kim,[79] J. Lee,[79] S. W. Lee,[79] C. S. Moon,[79] Y. D. Oh,[79] S. I. Pak,[79] S. Sekmen,[79] D. C. Son,[79] Y. C. Yang,[79] H. Kim,[80] D. H. Moon,[80] G. Oh,[80] B. Francois,[81] J. Goh,[81,ii] T. J. Kim,[81] S. Cho,[82]

S. Choi,[82] Y. Go,[82] D. Gyun,[82] S. Ha,[82] B. Hong,[82] Y. Jo,[82] K. Lee,[82] K. S. Lee,[82] S. Lee,[82] J. Lim,[82] S. K. Park,[82] Y. Roh,[82] H. S. Kim,[83] J. Almond,[84] J. Kim,[84] J. S. Kim,[84] H. Lee,[84] K. Lee,[84] S. Lee,[84] K. Nam,[84] S. B. Oh,[84] B. C. Radburn-Smith,[84] S. h. Seo,[84] U. K. Yang,[84] H. D. Yoo,[84] G. B. Yu,[84] D. Jeon,[85] H. Kim,[85] J. H. Kim,[85] J. S. H. Lee,[85] I. C. Park,[85] Y. Choi,[86] C. Hwang,[86] J. Lee,[86] I. Yu,[86] V. Veckalns,[87,jj] V. Dudenas,[88] A. Juodagalvis,[88] J. Vaitkus,[88] Z. A. Ibrahim,[89] M. A. B. Md Ali,[89,kk] F. Mohamad Idris,[89,ll] W. A. T. Wan Abdullah,[89] M. N. Yusli,[89] Z. Zolkapli,[89] J. F. Benitez,[90] A. Castaneda Hernandez,[90] J. A. Murillo Quijada,[90] H. Castilla-Valdez,[91] E. De La Cruz-Burelo,[91] M. C. Duran-Osuna,[91] I. Heredia-De La Cruz,[91,mm] R. Lopez-Fernandez,[91] J. Mejia Guisao,[91] R. I. Rabadan-Trejo,[91] G. Ramirez-Sanchez,[91] R. Reyes-Almanza,[91] A. Sanchez-Hernandez,[91] S. Carrillo Moreno,[92] C. Oropeza Barrera,[92] M. Ramirez-Garcia,[92] F. Vazquez Valencia,[92] J. Eysermans,[93] I. Pedraza,[93] H. A. Salazar Ibarguen,[93] C. Uribe Estrada,[93] A. Morelos Pineda,[94] D. Krofcheck,[95] S. Bheesette,[96] P. H. Butler,[96] A. Ahmad,[97] M. Ahmad,[97] M. I. Asghar,[97] Q. Hassan,[97] H. R. Hoorani,[97] W. A. Khan,[97] M. A. Shah,[97] M. Shoaib,[97] M. Waqas,[97] H. Bialkowska,[98] M. Bluj,[98] B. Boimska,[98] T. Frueboes,[98] M. Górski,[98] M. Kazana,[98] M. Szleper,[98] P. Traczyk,[98] P. Zalewski,[98] K. Bunkowski,[99] A. Byszuk,[99,nn] K. Doroba,[99] A. Kalinowski,[99] M. Konecki,[99] J. Krolikowski,[99] M. Misiura,[99] M. Olszewski,[99] A. Pyskir,[99] M. Walczak,[99] M. Araujo,[100] P. Bargassa,[100] C. Beirão Da Cruz E Silva,[100] A. Di Francesco,[100] P. Faccioli,[100] B. Galinhas,[100] M. Gallinaro,[100] J. Hollar,[100] N. Leonardo,[100] J. Seixas,[100] G. Strong,[100] O. Toldaiev,[100] J. Varela,[100] S. Afanasiev,[101] P. Bunin,[101] M. Gavrilenko,[101] I. Golutvin,[101] I. Gorbunov,[101] A. Kamenev,[101] V. Karjavine,[101] A. Lanev,[101] A. Malakhov,[101] V. Matveev,[101,oo,pp] P. Moisenz,[101] V. Palichik,[101] V. Perelygin,[101] S. Shmatov,[101] S. Shulha,[101] N. Skatchkov,[101] V. Smirnov,[101] N. Voytishin,[101] A. Zarubin,[101] V. Golovtsov,[102] Y. Ivanov,[102] V. Kim,[102,qq] E. Kuznetsova,[102,rr] P. Levchenko,[102] V. Murzin,[102] V. Oreshkin,[102] I. Smirnov,[102] D. Sosnov,[102] V. Sulimov,[102] L. Uvarov,[102] S. Vavilov,[102] A. Vorobyev,[102] Yu. Andreev,[103] A. Dermenev,[103] S. Gninenko,[103] N. Golubev,[103] A. Karneyeu,[103] M. Kirsanov,[103] N. Krasnikov,[103] A. Pashenkov,[103] A. Shabanov,[103] D. Tlisov,[103] A. Toropin,[103] V. Epshteyn,[104] V. Gavrilov,[104] N. Lychkovskaya,[104] V. Popov,[104] I. Pozdnyakov,[104] G. Safronov,[104] A. Spiridonov,[104] A. Stepennov,[104] V. Stolin,[104] M. Toms,[104] E. Vlasov,[104] A. Zhokin,[104] T. Aushev,[105] R. Chistov,[106,ss] M. Danilov,[106,ss] D. Philippov,[106] E. Tarkovskii,[106] V. Andreev,[107] M. Azarkin,[107] I. Dremin,[107,pp] M. Kirakosyan,[107] A. Terkulov,[107] A. Belyaev,[108] E. Boos,[108] V. Bunichev,[108] M. Dubinin,[108,tt] L. Dudko,[108] A. Ershov,[108] V. Klyukhin,[108] O. Kodolova,[108] I. Lokhtin,[108] S. Obraztsov,[108] M. Perfilov,[108] S. Petrushanko,[108] V. Savrin,[108] A. Barnyakov,[109,uu] V. Blinov,[109,uu] T. Dimova,[109,uu] L. Kardapoltsev,[109,uu] Y. Skovpen,[109,uu] I. Azhgirey,[110] I. Bayshev,[110] S. Bitioukov,[110] V. Kachanov,[110] A. Kalinin,[110] D. Konstantinov,[110] P. Mandrik,[110] V. Petrov,[110] R. Ryutin,[110] S. Slabospitskii,[110] A. Sobol,[110] S. Troshin,[110] N. Tyurin,[110] A. Uzunian,[110] A. Volkov,[110] A. Babaev,[111] S. Baidali,[111] V. Okhotnikov,[111] P. Adzic,[112,vv] P. Cirkovic,[112] D. Devetak,[112] M. Dordevic,[112] M. Milenovic,[112,ww] J. Milosevic,[112] J. Alcaraz Maestre,[113] A. Álvarez Fernández,[113] I. Bachiller,[113] M. Barrio Luna,[113] J. A. Brochero Cifuentes,[113] M. Cerrada,[113] N. Colino,[113] B. De La Cruz,[113] A. Delgado Peris,[113] C. Fernandez Bedoya,[113] J. P. Fernández Ramos,[113] J. Flix,[113] M. C. Fouz,[113] O. Gonzalez Lopez,[113] S. Goy Lopez,[113] J. M. Hernandez,[113] M. I. Josa,[113] D. Moran,[113] A. Pérez-Calero Yzquierdo,[113] J. Puerta Pelayo,[113] I. Redondo,[113] L. Romero,[113] S. Sánchez Navas,[113] M. S. Soares,[113] A. Triossi,[113] C. Albajar,[114] J. F. de Trocóniz,[114] J. Cuevas,[115] C. Erice,[115] J. Fernandez Menendez,[115] S. Folgueras,[115] I. Gonzalez Caballero,[115] J. R. González Fernández,[115] E. Palencia Cortezon,[115] V. Rodríguez Bouza,[115] S. Sanchez Cruz,[115] J. M. Vizan Garcia,[115] I. J. Cabrillo,[116] A. Calderon,[116] B. Chazin Quero,[116] J. Duarte Campderros,[116] M. Fernandez,[116] P. J. Fernández Manteca,[116] A. García Alonso,[116] J. Garcia-Ferrero,[116] G. Gomez,[116] A. Lopez Virto,[116] J. Marco,[116] C. Martinez Rivero,[116] P. Martinez Ruiz del Arbol,[116] F. Matorras,[116] J. Piedra Gomez,[116] C. Prieels,[116] T. Rodrigo,[116] A. Ruiz-Jimeno,[116] L. Scodellaro,[116] N. Trevisani,[116] I. Vila,[116] R. Vilar Cortabitarte,[116] N. Wickramage,[117] D. Abbaneo,[118] B. Akgun,[118] E. Auffray,[118] G. Auzinger,[118] P. Baillon,[118] A. H. Ball,[118] D. Barney,[118] J. Bendavid,[118] M. Bianco,[118] A. Bocci,[118] C. Botta,[118] E. Brondolin,[118] T. Camporesi,[118] M. Cepeda,[118] G. Cerminara,[118] E. Chapon,[118] Y. Chen,[118] G. Cucciati,[118] D. d'Enterria,[118] A. Dabrowski,[118] N. Daci,[118] V. Daponte,[118] A. David,[118] A. De Roeck,[118] N. Deelen,[118] M. Dobson,[118] M. Dünser,[118] N. Dupont,[118] A. Elliott-Peisert,[118] F. Fallavollita,[118,xx] D. Fasanella,[118] G. Franzoni,[118] J. Fulcher,[118] W. Funk,[118] D. Gigi,[118] A. Gilbert,[118] K. Gill,[118] F. Glege,[118] M. Gruchala,[118] M. Guilbaud,[118] D. Gulhan,[118] J. Hegeman,[118] C. Heidegger,[118] Y. Iiyama,[118] V. Innocente,[118] G. M. Innocenti,[118] A. Jafari,[118] P. Janot,[118] O. Karacheban,[118,u] J. Kieseler,[118] A. Kornmayer,[118] M. Krammer,[118,b] C. Lange,[118] P. Lecoq,[118] C. Lourenço,[118] L. Malgeri,[118] M. Mannelli,[118] A. Massironi,[118] F. Meijers,[118] J. A. Merlin,[118] S. Mersi,[118] E. Meschi,[118] F. Moortgat,[118] M. Mulders,[118] J. Ngadiuba,[118] S. Nourbakhsh,[118] S. Orfanelli,[118] L. Orsini,[118] F. Pantaleo,[118,r] L. Pape,[118] E. Perez,[118] M. Peruzzi,[118] A. Petrilli,[118] G. Petrucciani,[118] A. Pfeiffer,[118] M. Pierini,[118] F. M. Pitters,[118] D. Rabady,[118] A. Racz,[118]

M. Rovere,[118] H. Sakulin,[118] C. Schäfer,[118] C. Schwick,[118] M. Selvaggi,[118] A. Sharma,[118] P. Silva,[118] P. Sphicas,[118,yy] A. Stakia,[118] J. Steggemann,[118] D. Treille,[118] A. Tsirou,[118] A. Vartak,[118] M. Verzetti,[118] W. D. Zeuner,[118] L. Caminada,[119,zz] K. Deiters,[119] W. Erdmann,[119] R. Horisberger,[119] Q. Ingram,[119] H. C. Kaestli,[119] D. Kotlinski,[119] U. Langenegger,[119] T. Rohe,[119] S. A. Wiederkehr,[119] M. Backhaus,[120] L. Bäni,[120] P. Berger,[120] N. Chernyavskaya,[120] G. Dissertori,[120] M. Dittmar,[120] M. Donegà,[120] C. Dorfer,[120] T. A. Gómez Espinosa,[120] C. Grab,[120] D. Hits,[120] T. Klijnsma,[120] W. Lustermann,[120] R. A. Manzoni,[120] M. Marionneau,[120] M. T. Meinhard,[120] F. Micheli,[120] P. Musella,[120] F. Nessi-Tedaldi,[120] F. Pauss,[120] G. Perrin,[120] L. Perrozzi,[120] S. Pigazzini,[120] M. Reichmann,[120] C. Reissel,[120] D. Ruini,[120] D. A. Sanz Becerra,[120] M. Schönenberger,[120] L. Shchutska,[120] V. R. Tavolaro,[120] K. Theofilatos,[120] M. L. Vesterbacka Olsson,[120] R. Wallny,[120] D. H. Zhu,[120] T. K. Aarrestad,[121] C. Amsler,[121,aaa] D. Brzhechko,[121] M. F. Canelli,[121] A. De Cosa,[121] R. Del Burgo,[121] S. Donato,[121] C. Galloni,[121] T. Hreus,[121] B. Kilminster,[121] S. Leontsinis,[121] V. M. Mikuni,[121] I. Neutelings,[121] G. Rauco,[121] P. Robmann,[121] D. Salerno,[121] K. Schweiger,[121] C. Seitz,[121] Y. Takahashi,[121] S. Wertz,[121] A. Zucchetta,[121] T. H. Doan,[122] C. M. Kuo,[122] W. Lin,[122] S. S. Yu,[122] P. Chang,[123] Y. Chao,[123] K. F. Chen,[123] P. H. Chen,[123] W.-S. Hou,[123] Y. F. Liu,[123] R.-S. Lu,[123] E. Paganis,[123] A. Psallidas,[123] A. Steen,[123] B. Asavapibhop,[124] N. Srimanobhas,[124] N. Suwonjandee,[124] A. Bat,[125] F. Boran,[125] S. Damarseckin,[125] Z. S. Demiroglu,[125] F. Dolek,[125] C. Dozen,[125] I. Dumanoglu,[125] E. Eskut,[125] G. Gokbulut,[125] Emine Gurpinar Guler,[125,bbb] Y. Guler,[125] I. Hos,[125,ccc] C. Isik,[125] E. E. Kangal,[125,ddd] O. Kara,[125] A. Kayis Topaksu,[125] U. Kiminsu,[125] M. Oglakci,[125] G. Onengut,[125] K. Ozdemir,[125,eee] S. Ozturk,[125,fff] A. Polatoz,[125] D. Sunar Cerci,[125,ggg] U. G. Tok,[125] S. Turkcapar,[125] I. S. Zorbakir,[125] C. Zorbilmez,[125] B. Isildak,[126,hhh] G. Karapinar,[126,iii] M. Yalvac,[126] M. Zeyrek,[126] I. O. Atakisi,[127] E. Gülmez,[127] M. Kaya,[127,jjj] O. Kaya,[127,kkk] Ö. Özçelik,[127] S. Ozkorucuklu,[127,lll] S. Tekten,[127] E. A. Yetkin,[127,mmm] M. N. Agaras,[128] A. Cakir,[128] K. Cankocak,[128] Y. Komurcu,[128] S. Sen,[128,nnn] B. Grynyov,[129] L. Levchuk,[130] F. Ball,[131] J. J. Brooke,[131] D. Burns,[131] E. Clement,[131] D. Cussans,[131] O. Davignon,[131] H. Flacher,[131] J. Goldstein,[131] G. P. Heath,[131] H. F. Heath,[131] L. Kreczko,[131] D. M. Newbold,[131,ooo] S. Paramesvaran,[131] B. Penning,[131] T. Sakuma,[131] D. Smith,[131] V. J. Smith,[131] J. Taylor,[131] A. Titterton,[131] K. W. Bell,[132] A. Belyaev,[132,ppp] C. Brew,[132] R. M. Brown,[132] D. Cieri,[132] D. J. A. Cockerill,[132] J. A. Coughlan,[132] K. Harder,[132] S. Harper,[132] J. Linacre,[132] K. Manolopoulos,[132] E. Olaiya,[132] D. Petyt,[132] T. Reis,[132] T. Schuh,[132] C. H. Shepherd-Themistocleous,[132] A. Thea,[132] I. R. Tomalin,[132] T. Williams,[132] W. J. Womersley,[132] R. Bainbridge,[133] P. Bloch,[133] J. Borg,[133] S. Breeze,[133] O. Buchmuller,[133] A. Bundock,[133] D. Colling,[133] P. Dauncey,[133] G. Davies,[133] M. Della Negra,[133] R. Di Maria,[133] P. Everaerts,[133] G. Hall,[133] G. Iles,[133] T. James,[133] M. Komm,[133] C. Laner,[133] L. Lyons,[133] A.-M. Magnan,[133] S. Malik,[133] A. Martelli,[133] V. Milosevic,[133] J. Nash,[133,qqq] A. Nikitenko,[133,h] V. Palladino,[133] M. Pesaresi,[133] D. M. Raymond,[133] A. Richards,[133] A. Rose,[133] E. Scott,[133] C. Seez,[133] A. Shtipliyski,[133] G. Singh,[133] M. Stoye,[133] T. Strebler,[133] S. Summers,[133] A. Tapper,[133] K. Uchida,[133] T. Virdee,[133,r] N. Wardle,[133] D. Winterbottom,[133] J. Wright,[133] S. C. Zenz,[133] J. E. Cole,[134] P. R. Hobson,[134] A. Khan,[134] P. Kyberd,[134] C. K. Mackay,[134] A. Morton,[134] I. D. Reid,[134] L. Teodorescu,[134] S. Zahid,[134] K. Call,[135] J. Dittmann,[135] K. Hatakeyama,[135] H. Liu,[135] C. Madrid,[135] B. McMaster,[135] N. Pastika,[135] C. Smith,[135] R. Bartek,[136] A. Dominguez,[136] A. Buccilli,[137] O. Charaf,[137] S. I. Cooper,[137] C. Henderson,[137] P. Rumerio,[137] C. West,[137] D. Arcaro,[138] T. Bose,[138] Z. Demiragli,[138] D. Gastler,[138] S. Girgis,[138] D. Pinna,[138] C. Richardson,[138] J. Rohlf,[138] D. Sperka,[138] I. Suarez,[138] L. Sulak,[138] D. Zou,[138] G. Benelli,[139] B. Burkle,[139] X. Coubez,[139] D. Cutts,[139] M. Hadley,[139] J. Hakala,[139] U. Heintz,[139] J. M. Hogan,[139,rrr] K. H. M. Kwok,[139] E. Laird,[139] G. Landsberg,[139] J. Lee,[139] Z. Mao,[139] M. Narain,[139] S. Sagir,[139,sss] R. Syarif,[139] E. Usai,[139] D. Yu,[139] R. Band,[140] C. Brainerd,[140] R. Breedon,[140] D. Burns,[140] M. Calderon De La Barca Sanchez,[140] M. Chertok,[140] J. Conway,[140] R. Conway,[140] P. T. Cox,[140] R. Erbacher,[140] C. Flores,[140] G. Funk,[140] W. Ko,[140] O. Kukral,[140] R. Lander,[140] M. Mulhearn,[140] D. Pellett,[140] J. Pilot,[140] S. Shalhout,[140] M. Shi,[140] D. Stolp,[140] D. Taylor,[140] K. Tos,[140] M. Tripathi,[140] Z. Wang,[140] F. Zhang,[140] M. Bachtis,[141] C. Bravo,[141] R. Cousins,[141] A. Dasgupta,[141] A. Florent,[141] J. Hauser,[141] M. Ignatenko,[141] N. Mccoll,[141] S. Regnard,[141] D. Saltzberg,[141] C. Schnaible,[141] V. Valuev,[141] E. Bouvier,[142] K. Burt,[142] R. Clare,[142] J. W. Gary,[142] S. M. A. Ghiasi Shirazi,[142] G. Hanson,[142] G. Karapostoli,[142] E. Kennedy,[142] F. Lacroix,[142] O. R. Long,[142] M. Olmedo Negrete,[142] M. I. Paneva,[142] W. Si,[142] L. Wang,[142] H. Wei,[142] S. Wimpenny,[142] B. R. Yates,[142] J. G. Branson,[143] P. Chang,[143] S. Cittolin,[143] M. Derdzinski,[143] R. Gerosa,[143] D. Gilbert,[143] B. Hashemi,[143] A. Holzner,[143] D. Klein,[143] G. Kole,[143] V. Krutelyov,[143] J. Letts,[143] M. Masciovecchio,[143] S. May,[143] D. Olivito,[143] S. Padhi,[143] M. Pieri,[143] V. Sharma,[143] M. Tadel,[143] J. Wood,[143] F. Würthwein,[143] A. Yagil,[143] G. Zevi Della Porta,[143] N. Amin,[144] R. Bhandari,[144] C. Campagnari,[144] M. Citron,[144] V. Dutta,[144] M. Franco Sevilla,[144] L. Gouskos,[144] R. Heller,[144] J. Incandela,[144] H. Mei,[144] A. Ovcharova,[144] H. Qu,[144] J. Richman,[144] D. Stuart,[144] S. Wang,[144] J. Yoo,[144] D. Anderson,[145] A. Bornheim,[145]

J. M. Lawhorn,[145] N. Lu,[145] H. B. Newman,[145] T. Q. Nguyen,[145] J. Pata,[145] M. Spiropulu,[145] J. R. Vlimant,[145] R. Wilkinson,[145] S. Xie,[145] Z. Zhang,[145] R. Y. Zhu,[145] M. B. Andrews,[146] T. Ferguson,[146] T. Mudholkar,[146] M. Paulini,[146] M. Sun,[146] I. Vorobiev,[146] M. Weinberg,[146] J. P. Cumalat,[147] W. T. Ford,[147] F. Jensen,[147] A. Johnson,[147] E. MacDonald,[147] T. Mulholland,[147] R. Patel,[147] A. Perloff,[147] K. Stenson,[147] K. A. Ulmer,[147] S. R. Wagner,[147] J. Alexander,[148] J. Chaves,[148] Y. Cheng,[148] J. Chu,[148] A. Datta,[148] K. Mcdermott,[148] N. Mirman,[148] J. Monroy,[148] J. R. Patterson,[148] D. Quach,[148] A. Rinkevicius,[148] A. Ryd,[148] L. Skinnari,[148] L. Soffi,[148] S. M. Tan,[148] Z. Tao,[148] J. Thom,[148] J. Tucker,[148] P. Wittich,[148] M. Zientek,[148] S. Abdullin,[149] M. Albrow,[149] M. Alyari,[149] G. Apollinari,[149] A. Apresyan,[149] A. Apyan,[149] S. Banerjee,[149] L. A. T. Bauerdick,[149] A. Beretvas,[149] J. Berryhill,[149] P. C. Bhat,[149] K. Burkett,[149] J. N. Butler,[149] A. Canepa,[149] G. B. Cerati,[149] H. W. K. Cheung,[149] F. Chlebana,[149] M. Cremonesi,[149] J. Duarte,[149] V. D. Elvira,[149] J. Freeman,[149] Z. Gecse,[149] E. Gottschalk,[149] L. Gray,[149] D. Green,[149] S. Grünendahl,[149] O. Gutsche,[149] J. Hanlon,[149] R. M. Harris,[149] S. Hasegawa,[149] J. Hirschauer,[149] Z. Hu,[149] B. Jayatilaka,[149] S. Jindariani,[149] M. Johnson,[149] U. Joshi,[149] B. Klima,[149] M. J. Kortelainen,[149] B. Kreis,[149] S. Lammel,[149] D. Lincoln,[149] R. Lipton,[149] M. Liu,[149] T. Liu,[149] J. Lykken,[149] K. Maeshima,[149] J. M. Marraffino,[149] D. Mason,[149] P. McBride,[149] P. Merkel,[149] S. Mrenna,[149] S. Nahn,[149] V. O'Dell,[149] K. Pedro,[149] C. Pena,[149] O. Prokofyev,[149] G. Rakness,[149] F. Ravera,[149] A. Reinsvold,[149] L. Ristori,[149] A. Savoy-Navarro,[149,ttt] B. Schneider,[149] E. Sexton-Kennedy,[149] A. Soha,[149] W. J. Spalding,[149] L. Spiegel,[149] S. Stoynev,[149] J. Strait,[149] N. Strobbe,[149] L. Taylor,[149] S. Tkaczyk,[149] N. V. Tran,[149] L. Uplegger,[149] E. W. Vaandering,[149] C. Vernieri,[149] M. Verzocchi,[149] R. Vidal,[149] M. Wang,[149] H. A. Weber,[149] D. Acosta,[150] P. Avery,[150] P. Bortignon,[150] D. Bourilkov,[150] A. Brinkerhoff,[150] L. Cadamuro,[150] A. Carnes,[150] D. Curry,[150] R. D. Field,[150] S. V. Gleyzer,[150] B. M. Joshi,[150] J. Konigsberg,[150] A. Korytov,[150] K. H. Lo,[150] P. Ma,[150] K. Matchev,[150] N. Menendez,[150] G. Mitselmakher,[150] D. Rosenzweig,[150] K. Shi,[150] J. Wang,[150] S. Wang,[150] X. Zuo,[150] Y. R. Joshi,[151] S. Linn,[151] A. Ackert,[152] T. Adams,[152] A. Askew,[152] S. Hagopian,[152] V. Hagopian,[152] K. F. Johnson,[152] R. Khurana,[152] T. Kolberg,[152] G. Martinez,[152] T. Perry,[152] H. Prosper,[152] A. Saha,[152] C. Schiber,[152] R. Yohay,[152] M. M. Baarmand,[153] V. Bhopatkar,[153] S. Colafranceschi,[153] M. Hohlmann,[153] D. Noonan,[153] M. Rahmani,[153] T. Roy,[153] M. Saunders,[153] F. Yumiceva,[153] M. R. Adams,[154] L. Apanasevich,[154] D. Berry,[154] R. R. Betts,[154] R. Cavanaugh,[154] X. Chen,[154] S. Dittmer,[154] O. Evdokimov,[154] C. E. Gerber,[154] D. A. Hangal,[154] D. J. Hofman,[154] K. Jung,[154] J. Kamin,[154] C. Mills,[154] M. B. Tonjes,[154] N. Varelas,[154] H. Wang,[154] X. Wang,[154] Z. Wu,[154] J. Zhang,[154] M. Alhusseini,[155] B. Bilki,[155,bbb] W. Clarida,[155] K. Dilsiz,[155,uuu] S. Durgut,[155] R. P. Gandrajula,[155] M. Haytmyradov,[155] V. Khristenko,[155] O. K. Köseyan,[155] J.-P. Merlo,[155] A. Mestvirishvili,[155] A. Moeller,[155] J. Nachtman,[155] H. Ogul,[155,vvv] Y. Onel,[155] F. Ozok,[155,www] A. Penzo,[155] C. Snyder,[155] E. Tiras,[155] J. Wetzel,[155] B. Blumenfeld,[156] A. Cocoros,[156] N. Eminizer,[156] D. Fehling,[156] L. Feng,[156] A. V. Gritsan,[156] W. T. Hung,[156] P. Maksimovic,[156] J. Roskes,[156] U. Sarica,[156] M. Swartz,[156] M. Xiao,[156] A. Al-bataineh,[157] P. Baringer,[157] A. Bean,[157] S. Boren,[157] J. Bowen,[157] A. Bylinkin,[157] J. Castle,[157] S. Khalil,[157] A. Kropivnitskaya,[157] D. Majumder,[157] W. Mcbrayer,[157] M. Murray,[157] C. Rogan,[157] S. Sanders,[157] E. Schmitz,[157] J. D. Tapia Takaki,[157] Q. Wang,[157] S. Duric,[158] A. Ivanov,[158] K. Kaadze,[158] D. Kim,[158] Y. Maravin,[158] D. R. Mendis,[158] T. Mitchell,[158] A. Modak,[158] A. Mohammadi,[158] F. Rebassoo,[159] D. Wright,[159] A. Baden,[160] O. Baron,[160] A. Belloni,[160] S. C. Eno,[160] Y. Feng,[160] C. Ferraioli,[160] N. J. Hadley,[160] S. Jabeen,[160] G. Y. Jeng,[160] R. G. Kellogg,[160] J. Kunkle,[160] A. C. Mignerey,[160] S. Nabili,[160] F. Ricci-Tam,[160] M. Seidel,[160] Y. H. Shin,[160] A. Skuja,[160] S. C. Tonwar,[160] K. Wong,[160] D. Abercrombie,[161] B. Allen,[161] V. Azzolini,[161] A. Baty,[161] R. Bi,[161] S. Brandt,[161] W. Busza,[161] I. A. Cali,[161] M. D'Alfonso,[161] G. Gomez Ceballos,[161] M. Goncharov,[161] P. Harris,[161] D. Hsu,[161] M. Hu,[161] M. Klute,[161] D. Kovalskyi,[161] Y.-J. Lee,[161] P. D. Luckey,[161] B. Maier,[161] A. C. Marini,[161] C. Mcginn,[161] C. Mironov,[161] S. Narayanan,[161] X. Niu,[161] C. Paus,[161] D. Rankin,[161] C. Roland,[161] G. Roland,[161] Z. Shi,[161] G. S. F. Stephans,[161] K. Sumorok,[161] K. Tatar,[161] D. Velicanu,[161] J. Wang,[161] T. W. Wang,[161] B. Wyslouch,[161] A. C. Benvenuti,[162,a] R. M. Chatterjee,[162] A. Evans,[162] P. Hansen,[162] J. Hiltbrand,[162] Sh. Jain,[162] S. Kalafut,[162] M. Krohn,[162] Y. Kubota,[162] Z. Lesko,[162] J. Mans,[162] R. Rusack,[162] M. A. Wadud,[162] J. G. Acosta,[163] S. Oliveros,[163] E. Avdeeva,[164] K. Bloom,[164] D. R. Claes,[164] C. Fangmeier,[164] L. Finco,[164] F. Golf,[164] R. Gonzalez Suarez,[164] R. Kamalieddin,[164] I. Kravchenko,[164] J. E. Siado,[164] G. R. Snow,[164] B. Stieger,[164] A. Godshalk,[165] C. Harrington,[165] I. Iashvili,[165] A. Kharchilava,[165] C. Mclean,[165] D. Nguyen,[165] A. Parker,[165] S. Rappoccio,[165] B. Roozbahani,[165] G. Alverson,[166] E. Barberis,[166] C. Freer,[166] Y. Haddad,[166] A. Hortiangtham,[166] G. Madigan,[166] D. M. Morse,[166] T. Orimoto,[166] A. Tishelman-charny,[166] T. Wamorkar,[166] B. Wang,[166] A. Wisecarver,[166] D. Wood,[166] S. Bhattacharya,[167] J. Bueghly,[167] T. Gunter,[167] K. A. Hahn,[167] N. Odell,[167] M. H. Schmitt,[167] K. Sung,[167] M. Trovato,[167] M. Velasco,[167] R. Bucci,[168] N. Dev,[168] R. Goldouzian,[168] M. Hildreth,[168] K. Hurtado Anampa,[168] C. Jessop,[168] D. J. Karmgard,[168] K. Lannon,[168] W. Li,[168] N. Loukas,[168] N. Marinelli,[168] F. Meng,[168] C. Mueller,[168]

Y. Musienko,[168,oo] M. Planer,[168] R. Ruchti,[168] P. Siddireddy,[168] G. Smith,[168] S. Taroni,[168] M. Wayne,[168] A. Wightman,[168] M. Wolf,[168] A. Woodard,[168] J. Alimena,[169] L. Antonelli,[169] B. Bylsma,[169] L. S. Durkin,[169] S. Flowers,[169] B. Francis,[169] C. Hill,[169] W. Ji,[169] A. Lefeld,[169] T. Y. Ling,[169] W. Luo,[169] B. L. Winer,[169] S. Cooperstein,[170] G. Dezoort,[170] P. Elmer,[170] J. Hardenbrook,[170] N. Haubrich,[170] S. Higginbotham,[170] A. Kalogeropoulos,[170] S. Kwan,[170] D. Lange,[170] M. T. Lucchini,[170] J. Luo,[170] D. Marlow,[170] K. Mei,[170] I. Ojalvo,[170] J. Olsen,[170] C. Palmer,[170] P. Piroué,[170] J. Salfeld-Nebgen,[170] D. Stickland,[170] C. Tully,[170] S. Malik,[171] S. Norberg,[171] A. Barker,[172] V. E. Barnes,[172] S. Das,[172] L. Gutay,[172] M. Jones,[172] A. W. Jung,[172] A. Khatiwada,[172] B. Mahakud,[172] D. H. Miller,[172] N. Neumeister,[172] C. C. Peng,[172] S. Piperov,[172] H. Qiu,[172] J. F. Schulte,[172] J. Sun,[172] F. Wang,[172] R. Xiao,[172] W. Xie,[172] T. Cheng,[173] J. Dolen,[173] N. Parashar,[173] Z. Chen,[174] K. M. Ecklund,[174] S. Freed,[174] F. J. M. Geurts,[174] M. Kilpatrick,[174] Arun Kumar,[174] W. Li,[174] B. P. Padley,[174] R. Redjimi,[174] J. Roberts,[174] J. Rorie,[174] W. Shi,[174] Z. Tu,[174] A. Zhang,[174] A. Bodek,[175] P. de Barbaro,[175] R. Demina,[175] Y. t. Duh,[175] J. L. Dulemba,[175] C. Fallon,[175] T. Ferbel,[175] M. Galanti,[175] A. Garcia-Bellido,[175] J. Han,[175] O. Hindrichs,[175] A. Khukhunaishvili,[175] E. Ranken,[175] P. Tan,[175] R. Taus,[175] B. Chiarito,[176] J. P. Chou,[176] Y. Gershtein,[176] E. Halkiadakis,[176] A. Hart,[176] M. Heindl,[176] E. Hughes,[176] S. Kaplan,[176] R. Kunnawalkam Elayavalli,[176] S. Kyriacou,[176] I. Laflotte,[176] A. Lath,[176] R. Montalvo,[176] K. Nash,[176] M. Osherson,[176] H. Saka,[176] S. Salur,[176] S. Schnetzer,[176] D. Sheffield,[176] S. Somalwar,[176] R. Stone,[176] S. Thomas,[176] P. Thomassen,[176] H. Acharya,[177] A. G. Delannoy,[177] J. Heideman,[177] G. Riley,[177] S. Spanier,[177] O. Bouhali,[178,xxx] A. Celik,[178] M. Dalchenko,[178] M. De Mattia,[178] A. Delgado,[178] S. Dildick,[178] R. Eusebi,[178] J. Gilmore,[178] T. Huang,[178] T. Kamon,[178,yyy] S. Luo,[178] D. Marley,[178] R. Mueller,[178] D. Overton,[178] L. Perniè,[178] D. Rathjens,[178] A. Safonov,[178] N. Akchurin,[179] J. Damgov,[179] F. De Guio,[179] P. R. Dudero,[179] S. Kunori,[179] K. Lamichhane,[179] S. W. Lee,[179] T. Mengke,[179] S. Muthumuni,[179] T. Peltola,[179] S. Undleeb,[179] I. Volobouev,[179] Z. Wang,[179] A. Whitbeck,[179] S. Greene,[180] A. Gurrola,[180] R. Janjam,[180] W. Johns,[180] C. Maguire,[180] A. Melo,[180] H. Ni,[180] K. Padeken,[180] F. Romeo,[180] P. Sheldon,[180] S. Tuo,[180] J. Velkovska,[180] M. Verweij,[180] Q. Xu,[180] M. W. Arenton,[181] P. Barria,[181] B. Cox,[181] R. Hirosky,[181] M. Joyce,[181] A. Ledovskoy,[181] H. Li,[181] C. Neu,[181] Y. Wang,[181] E. Wolfe,[181] F. Xia,[181] R. Harr,[182] P. E. Karchin,[182] N. Poudyal,[182] J. Sturdy,[182] P. Thapa,[182] S. Zaleski,[182] J. Buchanan,[183] C. Caillol,[183] D. Carlsmith,[183] S. Dasu,[183] I. De Bruyn,[183] L. Dodd,[183] B. Gomber,[183,zzz] M. Grothe,[183] M. Herndon,[183] A. Hervé,[183] U. Hussain,[183] P. Klabbers,[183] A. Lanaro,[183] K. Long,[183] R. Loveless,[183] T. Ruggles,[183] A. Savin,[183] V. Sharma,[183] N. Smith,[183] W. H. Smith,[183] and N. Woods[183]

(CMS Collaboration)

[1]*Yerevan Physics Institute, Yerevan, Armenia*
[2]*Institut für Hochenergiephysik, Wien, Austria*
[3]*Institute for Nuclear Problems, Minsk, Belarus*
[4]*Universiteit Antwerpen, Antwerpen, Belgium*
[5]*Vrije Universiteit Brussel, Brussel, Belgium*
[6]*Université Libre de Bruxelles, Bruxelles, Belgium*
[7]*Ghent University, Ghent, Belgium*
[8]*Université Catholique de Louvain, Louvain-la-Neuve, Belgium*
[9]*Centro Brasileiro de Pesquisas Fisicas, Rio de Janeiro, Brazil*
[10]*Universidade do Estado do Rio de Janeiro, Rio de Janeiro, Brazil*
[11a]*Universidade Estadual Paulista, São Paulo, Brazil*
[11b]*Universidade Federal do ABC, São Paulo, Brazil*
[12]*Institute for Nuclear Research and Nuclear Energy, Bulgarian Academy of Sciences, Sofia, Bulgaria*
[13]*University of Sofia, Sofia, Bulgaria*
[14]*Beihang University, Beijing, China*
[15]*Institute of High Energy Physics, Beijing, China*
[16]*State Key Laboratory of Nuclear Physics and Technology, Peking University, Beijing, China*
[17]*Tsinghua University, Beijing, China*
[18]*Universidad de Los Andes, Bogota, Colombia*
[19]*University of Split, Faculty of Electrical Engineering, Mechanical Engineering and Naval Architecture, Split, Croatia*
[20]*University of Split, Faculty of Science, Split, Croatia*
[21]*Institute Rudjer Boskovic, Zagreb, Croatia*
[22]*University of Cyprus, Nicosia, Cyprus*
[23]*Charles University, Prague, Czech Republic*
[24]*Escuela Politecnica Nacional, Quito, Ecuador*

[25]*Universidad San Francisco de Quito, Quito, Ecuador*

[26]*Academy of Scientific Research and Technology of the Arab Republic of Egypt,*
Egyptian Network of High Energy Physics, Cairo, Egypt

[27]*National Institute of Chemical Physics and Biophysics, Tallinn, Estonia*

[28]*Department of Physics, University of Helsinki, Helsinki, Finland*

[29]*Helsinki Institute of Physics, Helsinki, Finland*

[30]*Lappeenranta University of Technology, Lappeenranta, Finland*

[31]*IRFU, CEA, Université Paris-Saclay, Gif-sur-Yvette, France*

[32]*Laboratoire Leprince-Ringuet, Ecole polytechnique, CNRS/IN2P3, Université Paris-Saclay,*
Palaiseau, France

[33]*Université de Strasbourg, CNRS, IPHC UMR 7178, Strasbourg, France*

[34]*Centre de Calcul de l'Institut National de Physique Nucleaire et de Physique des Particules,*
CNRS/IN2P3, Villeurbanne, France

[35]*Université de Lyon, Université Claude Bernard Lyon 1, CNRS-IN2P3,*
Institut de Physique Nucléaire de Lyon, Villeurbanne, France

[36]*Georgian Technical University, Tbilisi, Georgia*

[37]*Tbilisi State University, Tbilisi, Georgia*

[38]*RWTH Aachen University, I. Physikalisches Institut, Aachen, Germany*

[39]*RWTH Aachen University, III. Physikalisches Institut A, Aachen, Germany*

[40]*RWTH Aachen University, III. Physikalisches Institut B, Aachen, Germany*

[41]*Deutsches Elektronen-Synchrotron, Hamburg, Germany*

[42]*University of Hamburg, Hamburg, Germany*

[43]*Karlsruher Institut fuer Technologie, Karlsruhe, Germany*

[44]*Institute of Nuclear and Particle Physics (INPP), NCSR Demokritos, Aghia Paraskevi, Greece*

[45]*National and Kapodistrian University of Athens, Athens, Greece*

[46]*National Technical University of Athens, Athens, Greece*

[47]*University of Ioánnina, Ioánnina, Greece*

[48]*MTA-ELTE Lendület CMS Particle and Nuclear Physics Group, Eötvös Loránd University,*
Budapest, Hungary

[49]*Wigner Research Centre for Physics, Budapest, Hungary*

[50]*Institute of Nuclear Research ATOMKI, Debrecen, Hungary*

[51]*Institute of Physics, University of Debrecen, Debrecen, Hungary*

[52]*Indian Institute of Science (IISc), Bangalore, India*

[53]*National Institute of Science Education and Research, HBNI, Bhubaneswar, India*

[54]*Panjab University, Chandigarh, India*

[55]*University of Delhi, Delhi, India*

[56]*Saha Institute of Nuclear Physics, HBNI, Kolkata,India*

[57]*Indian Institute of Technology Madras, Madras, India*

[58]*Bhabha Atomic Research Centre, Mumbai, India*

[59]*Tata Institute of Fundamental Research-A, Mumbai, India*

[60]*Tata Institute of Fundamental Research-B, Mumbai, India*

[61]*Indian Institute of Science Education and Research (IISER), Pune, India*

[62]*Institute for Research in Fundamental Sciences (IPM), Tehran, Iran*

[63]*University College Dublin, Dublin, Ireland*

[64a]*INFN Sezione di Bari, Bari, Italy*

[64b]*Università di Bari, Bari, Italy*

[64c]*Politecnico di Bari, Bari, Italy*

[65a]*INFN Sezione di Bologna, Bologna, Italy*

[65b]*Università di Bologna, Bologna, Italy*

[66a]*INFN Sezione di Catania, Catania, Italy*

[66b]*Università di Catania, Catania, Italy*

[67a]*INFN Sezione di Firenze, Firenze, Italy*

[67b]*Università di Firenze, Firenze, Italy*

[68]*INFN Laboratori Nazionali di Frascati, Frascati, Italy*

[69a]*INFN Sezione di Genova, Genova, Italy*

[69b]*Università di Genova, Genova, Italy*

[70a]*INFN Sezione di Milano-Bicocca, Milano, Italy*

[70b]*Università di Milano-Bicocca, Milano, Italy*

[71a]*INFN Sezione di Napoli, Napoli, Italy*

[71b]*Università di Napoli 'Federico II', Napoli, Italy*

[71c]*Università della Basilicata, Potenza, Italy*
[71d]*Università G. Marconi, Roma, Italy*
[72a]*INFN Sezione di Padova, Padova, Italy*
[72b]*Università di Padova, Padova, Italy*
[72c]*Università di Trento, Trento, Italy*
[73a]*INFN Sezione di Pavia*
[73b]*Università di Pavia*
[74a]*INFN Sezione di Perugia, Perugia, Italy*
[74b]*Università di Perugia, Perugia, Italy*
[75a]*INFN Sezione di Pisa, Pisa, Italy*
[75b]*Università di Pisa, Pisa, Italy*
[75c]*Scuola Normale Superiore di Pisa, Pisa, Italy*
[76a]*INFN Sezione di Roma, Rome, Italy*
[76b]*Sapienza Università di Roma, Rome, Italy*
[77a]*INFN Sezione di Torino, Torino, Italy*
[77b]*Università di Torino, Torino, Italy*
[77c]*Università del Piemonte Orientale, Novara, Italy*
[78a]*INFN Sezione di Trieste, Trieste, Italy*
[78b]*Università di Trieste, Trieste, Italy*
[79]*Kyungpook National University, Daegu, Korea*
[80]*Chonnam National University, Institute for Universe and Elementary Particles, Kwangju, Korea*
[81]*Hanyang University, Seoul, Korea*
[82]*Korea University, Seoul, Korea*
[83]*Sejong University, Seoul, Korea*
[84]*Seoul National University, Seoul, Korea*
[85]*University of Seoul, Seoul, Korea*
[86]*Sungkyunkwan University, Suwon, Korea*
[87]*Riga Technical University, Riga, Latvia*
[88]*Vilnius University, Vilnius, Lithuania*
[89]*National Centre for Particle Physics, Universiti Malaya, Kuala Lumpur, Malaysia*
[90]*Universidad de Sonora (UNISON), Hermosillo, Mexico*
[91]*Centro de Investigacion y de Estudios Avanzados del IPN, Mexico City, Mexico*
[92]*Universidad Iberoamericana, Mexico City, Mexico*
[93]*Benemerita Universidad Autonoma de Puebla, Puebla, Mexico*
[94]*Universidad Autónoma de San Luis Potosí, San Luis Potosí, Mexico*
[95]*University of Auckland, Auckland, New Zealand*
[96]*University of Canterbury, Christchurch, New Zealand*
[97]*National Centre for Physics, Quaid-I-Azam University, Islamabad, Pakistan*
[98]*National Centre for Nuclear Research, Swierk, Poland*
[99]*Institute of Experimental Physics, Faculty of Physics, University of Warsaw, Warsaw, Poland*
[100]*Laboratório de Instrumentação e Física Experimental de Partículas, Lisboa, Portugal*
[101]*Joint Institute for Nuclear Research, Dubna, Russia*
[102]*Petersburg Nuclear Physics Institute, Gatchina (St. Petersburg), Russia*
[103]*Institute for Nuclear Research, Moscow, Russia*
[104]*Institute for Theoretical and Experimental Physics, Moscow, Russia*
[105]*Moscow Institute of Physics and Technology, Moscow, Russia*
[106]*National Research Nuclear University 'Moscow Engineering Physics Institute' (MEPhI),
Moscow, Russia*
[107]*P.N. Lebedev Physical Institute, Moscow, Russia*
[108]*Skobeltsyn Institute of Nuclear Physics, Lomonosov Moscow State University, Moscow, Russia*
[109]*Novosibirsk State University (NSU), Novosibirsk, Russia*
[110]*Institute for High Energy Physics of National Research Centre 'Kurchatov Institute', Protvino, Russia*
[111]*National Research Tomsk Polytechnic University, Tomsk, Russia*
[112]*University of Belgrade: Faculty of Physics and VINCA Institute of Nuclear Sciences*
[113]*Centro de Investigaciones Energéticas Medioambientales y Tecnológicas (CIEMAT), Madrid, Spain*
[114]*Universidad Autónoma de Madrid, Madrid, Spain*
[115]*Universidad de Oviedo, Oviedo, Spain*
[116]*Instituto de Física de Cantabria (IFCA), CSIC-Universidad de Cantabria, Santander, Spain*
[117]*University of Ruhuna, Department of Physics, Matara, Sri Lanka*
[118]*CERN, European Organization for Nuclear Research, Geneva, Switzerland*

[119]Paul Scherrer Institut, Villigen, Switzerland
[120]ETH Zurich—Institute for Particle Physics and Astrophysics (IPA), Zurich, Switzerland
[121]Universität Zürich, Zurich, Switzerland
[122]National Central University, Chung-Li, Taiwan
[123]National Taiwan University (NTU), Taipei, Taiwan
[124]Chulalongkorn University, Faculty of Science, Department of Physics, Bangkok, Thailand
[125]Çukurova University, Physics Department, Science and Art Faculty, Adana, Turkey
[126]Middle East Technical University, Physics Department, Ankara, Turkey
[127]Bogazici University, Istanbul, Turkey
[128]Istanbul Technical University, Istanbul, Turkey
[129]Institute for Scintillation Materials of National Academy of Science of Ukraine, Kharkov, Ukraine
[130]National Scientific Center, Kharkov Institute of Physics and Technology, Kharkov, Ukraine
[131]University of Bristol, Bristol, United Kingdom
[132]Rutherford Appleton Laboratory, Didcot, United Kingdom
[133]Imperial College, London, United Kingdom
[134]Brunel University, Uxbridge, United Kingdom
[135]Baylor University, Waco, Texas, USA
[136]Catholic University of America, Washington, DC, USA
[137]The University of Alabama, Tuscaloosa, Alabama, USA
[138]Boston University, Boston, Massachusetts, USA
[139]Brown University, Providence, Rhode Island, USA
[140]University of California at Davis, Davis, California, USA
[141]University of California at Los Angeles, Los Angeles, California, USA
[142]University of California, Riverside, Riverside, California, USA
[143]University of California at Riverside, San Diego, La Jolla, California, USA
[144]University of California at Santa Barbara, Santa Barbara—Department of Physics,
Santa Barbara, California, USA
[145]California Institute of Technology, Pasadena, California, USA
[146]Carnegie Mellon University, Pittsburgh, Pennsylvania, USA
[147]University of Colorado at Boulder, Boulder, Colorado, USA
[148]Cornell University, Ithaca, New York, USA
[149]Fermi National Accelerator Laboratory, Batavia, Illinois, USA
[150]University of Florida, Gainesville, Florida, USA
[151]Florida International University, Miami, Florida, USA
[152]Florida State University, Tallahassee, Florida, USA
[153]Florida Institute of Technology, Melbourne, Florida, USA
[154]University of Illinois at Chicago (UIC), Chicago, Illinois, USA
[155]The University of Iowa, Iowa City, Iowa, USA
[156]Johns Hopkins University, Baltimore, Maryland, USA
[157]The University of Kansas, Lawrence, Kansas, USA
[158]Kansas State University, Manhattan, Kansas, USA
[159]Lawrence Livermore National Laboratory, Livermore, California, USA
[160]University of Maryland, College Park, Maryland, USA
[161]Massachusetts Institute of Technology, Cambridge, Massachusetts, USA
[162]University of Minnesota, Minneapolis, Minnesota, USA
[163]University of Mississippi, Oxford, Mississippi, USA
[164]University of Nebraska-Lincoln, Lincoln, Nebraska, USA
[165]State University of New York at Buffalo, Buffalo, New York, USA
[166]Northeastern University, Boston, Massachusetts, USA
[167]Northwestern University, Evanston, Illinois, USA
[168]University of Notre Dame, Notre Dame, Indiana, USA
[169]The Ohio State University, Columbus, Ohio, USA
[170]Princeton University, Princeton, New Jersey, USA
[171]University of Puerto Rico, Mayaguez, Puerto Rico
[172]Purdue University, West Lafayette, Indiana, USA
[173]Purdue University Northwest, Hammond, Indiana, USA
[174]Rice University, Houston, Texas, USA
[175]University of Rochester, Rochester, New York, USA
[176]Rutgers, The State University of New Jersey, Piscataway, New Jersey, USA
[177]University of Tennessee, Knoxville, Tennessee, USA

[178]*Texas A&M University, College Station, Texas, USA*
[179]*Texas Tech University, Lubbock, Texas, USA*
[180]*Vanderbilt University, Nashville, Tennessee, USA*
[181]*University of Virginia, Charlottesville, Virginia, USA*
[182]*Wayne State University, Detroit, Michigan, USA*
[183]*University of Wisconsin—Madison, Madison, Wisconsin, USA*

[a]Deceased.
[b]Also at Vienna University of Technology, Vienna, Austria.
[c]Also at IRFU, CEA, Université Paris-Saclay, Gif-sur-Yvette, France.
[d]Also at Universidade Estadual de Campinas, Campinas, Brazil.
[e]Also at Federal University of Rio Grande do Sul, Porto Alegre, Brazil.
[f]Also at Université Libre de Bruxelles, Bruxelles, Belgium.
[g]Also at University of Chinese Academy of Sciences.
[h]Also at Institute for Theoretical and Experimental Physics, Moscow, Russia.
[i]Also at Joint Institute for Nuclear Research, Dubna, Russia.
[j]Also at Helwan University, Cairo, Egypt.
[k]Also at Zewail City of Science and Technology, Zewail, Egypt.
[l]Also at British University in Egypt, Cairo, Egypt.
[m]Also at Suez University, Suez, Egypt.
[n]Also at Fayoum University, El-Fayoum, Egypt.
[o]Also at Department of Physics, King Abdulaziz University, Jeddah, Saudi Arabia.
[p]Also at Université de Haute Alsace, Mulhouse, France.
[q]Also at Skobeltsyn Institute of Nuclear Physics, Lomonosov Moscow State University, Moscow, Russia.
[r]Also at CERN, European Organization for Nuclear Research, Geneva, Switzerland.
[s]Also at RWTH Aachen University, III. Physikalisches Institut A, Aachen, Germany.
[t]Also at University of Hamburg, Hamburg, Germany.
[u]Also at Brandenburg University of Technology, Cottbus, Germany.
[v]Also at Institute of Physics, University of Debrecen, Debrecen, Hungary.
[w]Also at Institute of Nuclear Research ATOMKI, Debrecen, Hungary.
[x]Also at MTA-ELTE Lendület CMS Particle and Nuclear Physics Group, Eötvös Loránd University, Budapest, Hungary.
[y]Also at IIT Bhubaneswar, Bhubaneswar, India.
[z]Also at Institute of Physics, Bhubaneswar, India.
[aa]Also at Shoolini University, Solan, India.
[bb]Also at University of Visva-Bharati, Santiniketan, India.
[cc]Also at Isfahan University of Technology, Isfahan, Iran.
[dd]Also at Plasma Physics Research Center, Science and Research Branch, Islamic Azad University, Tehran, Iran.
[ee]Also at ITALIAN NATIONAL AGENCY FOR NEW TECHNOLOGIES, ENERGY AND SUSTAINABLE ECONOMIC DEVELOPMENT, Bologna, Italy.
[ff]Also at CENTRO SICILIANO DI FISICA NUCLEARE E DI STRUTTURA DELLA MATERIA.
[gg]Also at Università degli Studi di Siena, Siena, Italy.
[hh]Also at Scuola Normale e Sezione dell'INFN, Pisa, Italy.
[ii]Also at Kyung Hee University, Department of Physics.
[jj]Also at Riga Technical University, Riga, Latvia.
[kk]Also at International Islamic University of Malaysia, Kuala Lumpur, Malaysia.
[ll]Also at Malaysian Nuclear Agency, MOSTI, Kajang, Malaysia.
[mm]Also at Consejo Nacional de Ciencia y Tecnología, Mexico City, Mexico.
[nn]Also at Warsaw University of Technology, Institute of Electronic Systems, Warsaw, Poland.
[oo]Also at Institute for Nuclear Research, Moscow, Russia.
[pp]Also at National Research Nuclear University 'Moscow Engineering Physics Institute' (MEPhI), Moscow, Russia.
[qq]Also at St. Petersburg State Polytechnical University, St. Petersburg, Russia.
[rr]Also at University of Florida, Gainesville, Florida, USA.
[ss]Also at P.N. Lebedev Physical Institute, Moscow, Russia.
[tt]Also at California Institute of Technology, Pasadena, California, USA.
[uu]Also at Budker Institute of Nuclear Physics, Novosibirsk, Russia.
[vv]Also at Faculty of Physics, University of Belgrade, Belgrade, Serbia.
[ww]Also at University of Belgrade: Faculty of Physics and VINCA Institute of Nuclear Sciences.
[xx]Also at INFN Sezione di Pavia, Università di Pavia, Pavia, Italy.
[yy]Also at National and Kapodistrian University of Athens, Athens, Greece.
[zz]Also at Universität Zürich, Zurich, Switzerland.

[aaa]Also at Stefan Meyer Institute for Subatomic Physics, Vienna, Austria.
[bbb]Also at Beykent University, Istanbul, Turkey.
[ccc]Also at Istanbul Aydin University, Istanbul, Turkey.
[ddd]Also at Mersin University, Mersin, Turkey.
[eee]Also at Piri Reis University, Istanbul, Turkey.
[fff]Also at Gaziosmanpasa University, Tokat, Turkey.
[ggg]Also at Adiyaman University, Adiyaman, Turkey.
[hhh]Also at Ozyegin University, Istanbul, Turkey.
[iii]Also at Izmir Institute of Technology, Izmir, Turkey.
[jjj]Also at Marmara University, Istanbul, Turkey.
[kkk]Also at Kafkas University, Kars, Turkey.
[lll]Also at Istanbul University, Istanbul, Turkey.
[mmm]Also at Istanbul Bilgi University, Istanbul, Turkey.
[nnn]Also at Hacettepe University, Ankara, Turkey.
[ooo]Also at Rutherford Appleton Laboratory, Didcot, United Kingdom.
[ppp]Also at School of Physics and Astronomy, University of Southampton, Southampton, United Kingdom.
[qqq]Also at Monash University, Faculty of Science, Clayton, Australia.
[rrr]Also at Bethel University, St. Paul, Minneapolis, USA.
[sss]Also at Karamanoğlu Mehmetbey University, Karaman, Turkey.
[ttt]Also at Purdue University, West Lafayette, Indiana, USA.
[uuu]Also at Bingol University, Bingol, Turkey.
[vvv]Also at Sinop University, Sinop, Turkey.
[www]Also at Mimar Sinan University, Istanbul, Istanbul, Turkey.
[xxx]Also at Texas A&M University at Qatar, Doha, Qatar.
[yyy]Also at Kyungpook National University, Daegu, Korea.
[zzz]Also at University of Hyderabad, Hyderabad, India.